Petrology, Vol. 10, No. 3, 2002, pp. 249–276. Translated from Petrologiya, Vol. 10, No. 3, 2002, pp. 283–311.
Original Russian Text Copyright © 2002 by Savko, Kal'mutskaya.
English Translation Copyright © 2002 by MAIK "Nauka/Interperiodica" (Russia).

Petrology of Potassium-Poor Metapelites of the Voronezh Crystalline Massif with Reference to the Olivine–Gedrite–Orthopyroxene–Garnet–Magnetite Assemblage

K. A. Savko and N. Yu. Kal'mutskaya

Voronezh State University, Universitetskaya pl. 1, Voronezh, 394693 Russia
e-mail: gfskig304@main.vsu.ru

Received October 9, 2001

Abstract—The central part of the Voronezh crystalline massif was determined to contain the following three petrochemical types of metapelites: (1) K-poor magnesian and aluminous cordierite–gedrite–anthophyllite schists, (2) K- and Al-rich muscovite–staurolite schists, and (3) K- and Al-poor Fe-rich grunerite–garnet rocks. A staurolite–sillimanite and a sillimanite–muscovite zone were mapped in the K-rich metapelites. The K-poor magnesian and aluminous metapelites are noted for the relations between the Fe mole fractions of their minerals: $Crd_{22–34} < Opx_{39.5} < Ath_{40–43} < Ged_{46–49} < Grt_{65–79}$. The assemblage of orthopyroxene with gedrite and garnet crystallized in the high-temperature part of the muscovite–sillimanite zone. The grunerite–garnet assemblage is stable in the metapelites of type 3 only within the Fe-rich region and does not overlap with other mineral equilibria. The rare mineral assemblage *Ol + Ged + Opx + Grt + Mag* of the K-poor moderately aluminous quartz-free metapelites was formed during regional metamorphism (T = 639°C, P = 4–5 kbar) at a combination of several factors: a specific bulk-rock chemistry (K-poor, moderately aluminous, and relatively highly magnesian quartz-free lithologies), metamorphic parameters (630°C and 4–5 kbar), and redox conditions (an elevated oxygen fugacity, above the quartz–fayalite–magnetite buffer). The P–T trajectory of the prograde metamorphic stage was controlled by the heating of the rocks from 530°C to approximately 630°C at pressures of 4–5 kbar.

INTRODUCTION

The succession of metamorphic facies and subfacies of metapelites (Korikovsky, 1979; Powell and Holland, 1990; Spear and Cheney; 1989, Xu *et al.*, 1994; and others) and metabasites (Dobretsov *et al.*, 1970; Ewans, 1990; Will *et al.*, 1998; and others) with increasing P–T parameters is known in fairly much detail. At the same time, metamorphic zoning was relatively rarely mapped in other rock types, such as iron-rich, magnesian, and potassium-poor gedrite–cordierite and grunerite–garnet varieties. Their successions of mineral assemblages are important for understanding the variations in phase equilibria with changing P–T conditions.

Cordierite–orthoamphibole rocks with ages from Archean to Middle Paleozoic are known on all continents. The unusual chemistry of orthoamphibole–cordierite rocks (high MgO, FeO, and Al_2O_3 concentrations at very low contents of CaO and K_2O), which has no analogues among igneous, sedimentary, and metamorphic rocks, stimulated numerous discussions about their nature. A detailed review of the main hypotheses of the origin of orthoamphibole–cordierite rocks, both "premetamorphic" and "synmetamorphic," was presented by Robinson *et al.* (1982). The former groups ("premetamorphic" hypotheses) relies on the isochemical character of the metamorphism and the specific chemistry of the protoliths, such as ancient weathering crusts (Tilley and Fleet, 1929; Gable and Sims, 1969; and others), evaporitic sediments (Schreuer and Abraham, 1976; Kamineni, 1979; Reinhardt, 1987; and others), and hydrothermally modified mafic and intermediate volcanics, which sometimes host sulfide ores (Easkola, 1914; Chinner and Fox, 1974; Glagolev and Boronikhin, 1977; Smith *et al.*, 1992; and others). The latter viewpoint is shared by most researchers. According to the other group of hypotheses ("synmetamorphic"), orthoamphibole–cordierite rocks result from a variety of synmetamorphic processes: metasomatic transformations of metapelites during their metamorphism (Schumacher and Robinson, 1987; Arnold and Sandiford, 1990; and others) or partial melting of these rocks with the development of cordierite–orthoamphibole restite (Grant, 1968; Hoffer and Grant, 1980).

It should be mentioned that, in spite of its nearly centenarian history, this issue remains unsettled as of yet, because even the REE fractionation of orthoamphibole–cordierite rocks in various areas shows significant differences (Smith *et al.*, 1992).

In potassium-poor magnesian and moderately aluminous metapelites of the Voronezh crystalline massif (VCM), which commonly contain the assemblage *Ged + Ath + Crd + Bt ± Sil ± Grt ± Opx ± Qtz* (whose anthophyllite and gedrite coexist as individual equilibrium phases), we also found the very rare quartz-free

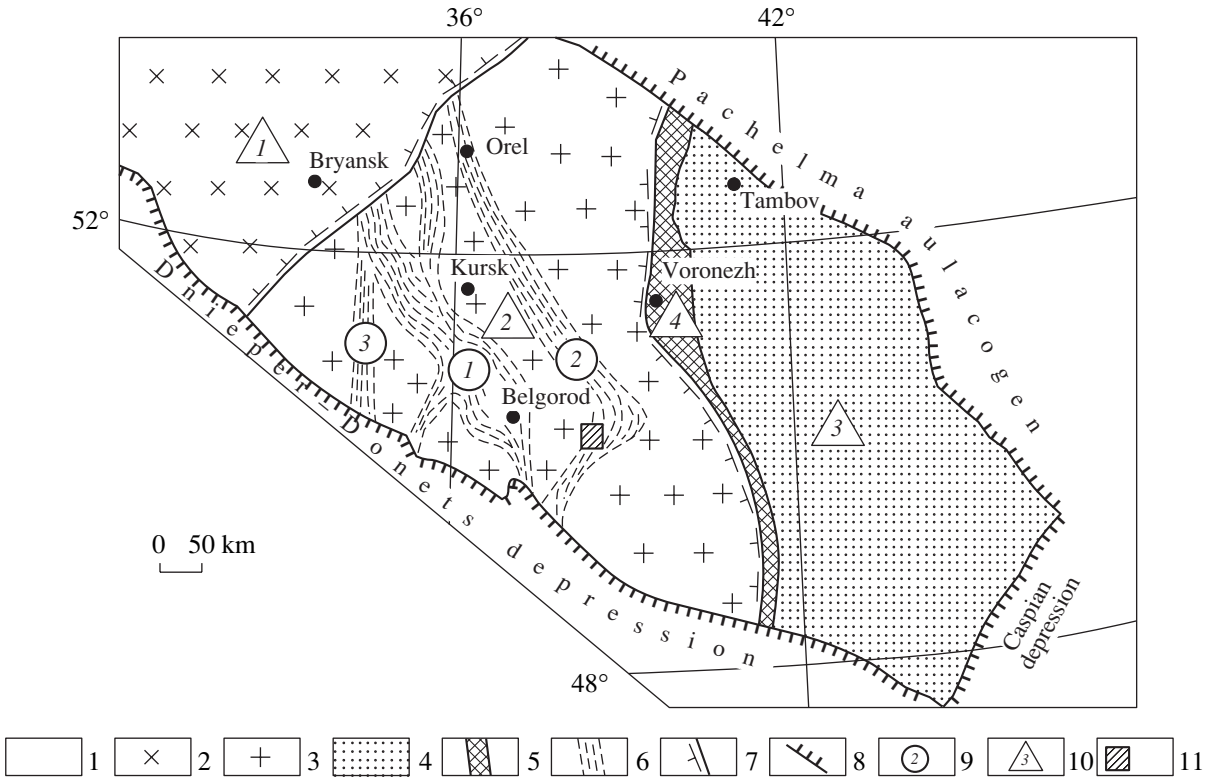

Fig. 1. Schematic tectonic map of the Voronezh crystalline massif (modified after N.M. Chernyshev, 1997).
Tectono–stratigraphic complexes: (1) platform, Riphean and Phanerozoic; (2–6) pre-Riphean: (2) Bryansk and Kursk megablocks, Early Archean consolidation, (4) Vorontsovskii foredeep, (5) Livny–Boguchary suture, (6) riftogenic structures of the second order; (7, 8) geologic boundaries: (7) between megablocks, (8) of the Voronezh crystalline massif; (9) riftogenic structures of the second order (circled numbers): (*1*) Belgorod–Mikhailovskaya, (*2*) Orel–Timskaya, (*3*) Krupetsko–Krivoi Rog; (10) structures of the first order (numbers in triangles): (*1*) Bryansk megablock, (*2*) Kursk megablock, (*3*) Voronezh megablock, (*4*) Livny–Boguchary suture; (11) Prioskol'skaya area (study area).

assemblage *Ol + Ged + Opx + Grt + Mag*.[1] Under the term *moderately aluminous metapelites*, we will understand rocks rich in alumina but bearing no aluminous minerals, such as alumina silicates and corundum. The bulk-rock compositions of moderately aluminous metapelites usually plot below the cordierite–garnet tie line in a Mg–Fe–Al plot, while highly aluminous metapelites lie above this line.

Our paper is devoted to phase equilibria in K-poor metapelites, including those with gedrite and olivine, and is focused on determining the parameters of their equilibrium coexistence. We compared the temperature zones and equilibria of orthoamphibole–cordierite schists and K-rich metapelites.

GEOLOGY

The Voronezh crystalline massif is a large basement uplift of the East European Platform with a relatively thin cover, 600 by 700 km in size. The massif is bounded by systems of graben-shaped aulacogens in the north and northeast (Pachelmskii, Moskovskii, Gzhatskii, and Toropets–Vyazemskii), the Dnieper–Donets depression in the south, the Orshansk depression in the west, and the Caspian depression in the east (Fig. 1).

The VCM is composed of structures of three main types: Early Archean gneiss–migmatite and granulite blocks, Late Archean granite–greenstone belts, and Early Proterozoic mobile belts around Early Archean blocks. In terms of metamorphism, the VCM is subdivided into Archean granulite (Bryansk and Kursk–Besedinskii) and unzoned migmatite–gneiss complexes (for example, Rossoshanskii); Late Archean and Early Proterozoic unzoned medium- and low-temperature complexes (Losevskaya Group and Voronezh Formation); and Early Proterozoic zonal complexes (Timskii and Vorontsovskii).

The Kursk block is an uplift of the Precambrian basement of the Voronezh crystalline massif between the Mikhailovskii–Belgorod and Orel–Timskii greenstone belts.

[1] Mineral symbols: *Ab* = albite, *An* = anorthite, *And* = andalusite, *Ath* = anthrophyllite; *Bt* = biotite, *Chl* = chlorite, *Crd* = cordierite, *En* = enstatite, *Ged* = gedrite, *Grt* = garnet, *Gru* = grunerite, *Kfs* = potassic feldspar, *Mag* = magnetite, *Ms* = muscovite, *Ol* = olivine, *Opx* = orthopyroxene, *Ort* = orthoclase, *Pl* = plagioclase, *Qtz* = quartz, *Sil* = sillimanite, *Spl* = spinel, *St* = staurolite, *Tlc* = talc.

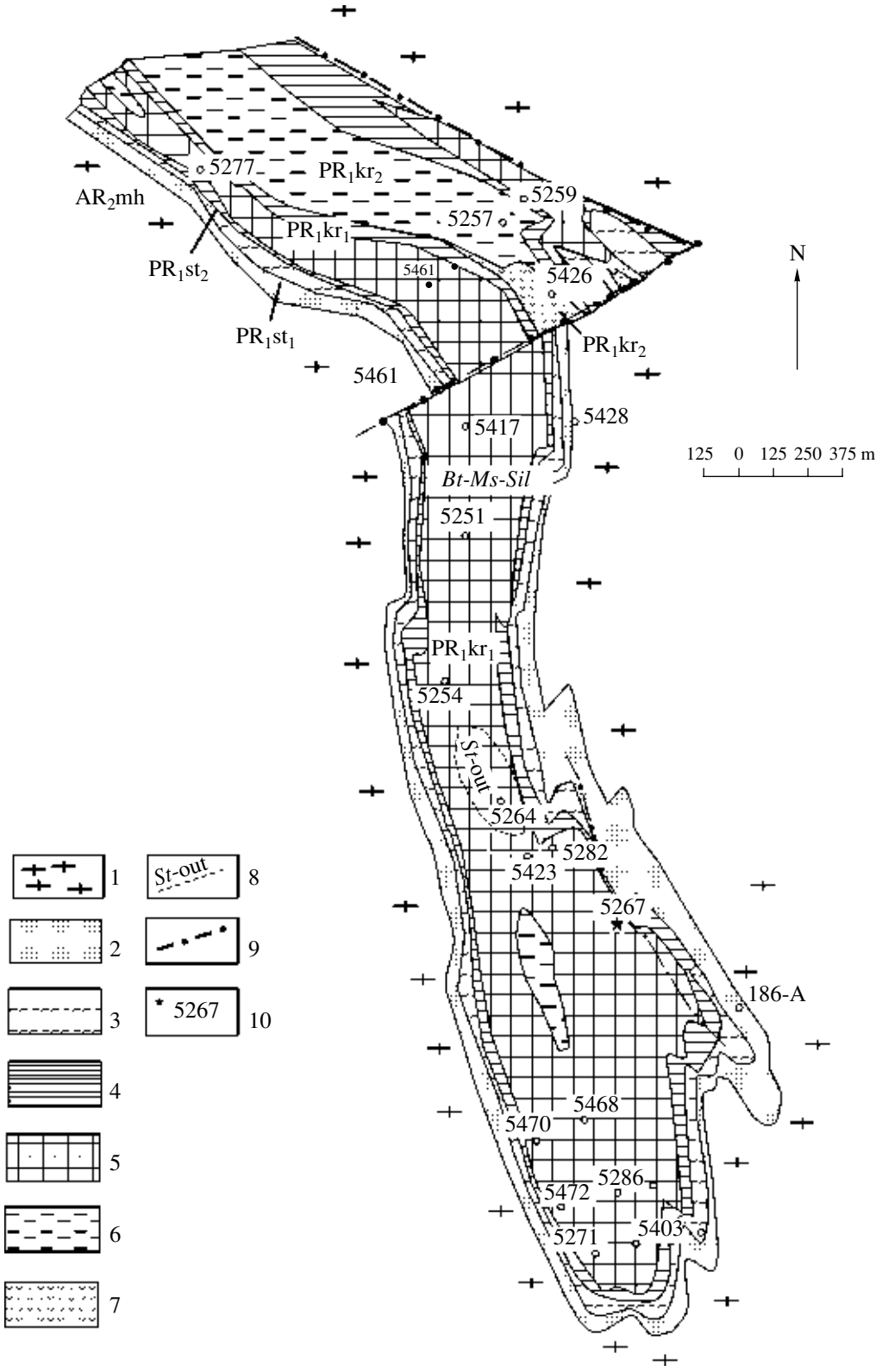

Fig. 2. Schematic geological map of the Prioskol'skaya area (modified after Shchegolev *et al.*, 1988).

(1, 2) Mikhailovskaya Group: (1) gneisses and schists, (2) amphibolites; (3–7) Kursk Group: (3, 4) Stoilensksya Formation (3—metasandstones, 4—schists), (5–7) Korobkovskaya Formation: (5—metapelites and barren or leanly mineralized Fe-quartzites, 6—mineralized Fe-quartzites and orthoamphibole–cordierite rocks, 7—overlying schists), (8) staurolite-out isograde; (9) faults; (10) hole that recovered rocks with the *Ol* + *Ged* + *Opx* + *Grt* + *Mag* assemblage.

The Prioskol'skaya structure (approximately 6 by 1 km) is spatially restricted to the southern closing of the Tim–Yastrebovskii continental rift.

The structure is composed of two lithostratigraphic complexes: the Late Archean Mikhailovskaya Group and the Early Proterozoic Kursk Group (Fig. 2). The Mikhailovskaya Group is represented by the Aleksandrovskaya Formation within the complex and consists of biotite, hornblende–biotite, and biotite–pyroxene–hornblende gneisses; chlorite–amphibole and plagioclase–biotite schists; and amphibolites. The Mikhailovskaya and Kursk groups are separated by a stratigraphic unconformity with basal conglomerates and metamorphosed weathering crusts in the stratigraphic succession.

The Kursk Group consists of the Stoilenskaya and Korobkovskaya formations. The rocks of the Stoilenskaya Formation are mostly quartz–mica schists, metamorphosed sandstones and, in zones of high-temperature metamorphism, gneisses. The Korobkovskaya Formation is dominated by Fe-quartzites. The thickness of the Kursk Group is 80–110 m. The orthoamphibole–cordierite rocks described in this paper belong to the Kursk Group of Early Proterozoic age.

Within the Prioskol'skaya structure, the thickens of the unmetamorphosed Phanerozoic sedimentary cover, resting on Precambrian rocks, varies from 60 to 132 m.

PETROGRAPHY

The mineralogical composition of metapelites (Ca-poor rocks) is determined by their K and Al concentrations. K_2O-rich metapelites contain muscovite and, after its high-temperature decomposition, potassic feldspar. K_2O-poor rocks have neither muscovite nor potassic feldspar, and their only K-bearing mineral is biotite. This type of metapelites bears Ca-free amphiboles (gedrite, anthophyllite, and grunerite), which become unstable in the presence of excess muscovite and potassic feldspar (Korikovsky, 1979). If the rocks are relatively high in MgO, they also contain sillimanite, staurolite, and cordierite, and their amphiboles are anthophyllite and gedrite. K- and Al-poor Fe-rich varieties contain grunerite and almandine-rich garnet. The instability of Ca-free amphiboles in K-rich rocks is explained by the fact that excess K_2O causes the presence of biotite.

The metapelites of the Prioskol'skaya structure are gray, light gray, and greenish gray fine-, medium-, or coarse-grained schists and gneisses of variable composition. They can be subdivided into three petrochemical types with different mineral assemblages:

(1) K_2O-poor, relatively magnesian and moderately aluminous cordierite–gedrite–anthophyllite schists, whose typical assemblage is *Ged + Ath + Crd + Grt* with more rare *Qtz*, *Bt*, *Opx*, and *Sil*;

(2) K_2O-rich metapelites, whose characteristic assemblages are *Qtz + Pl + St + Bt + Sil + Grt* and *Qtz + Bt + Ms + Sil + And + Spl + Kfs* (Table 1);

(3) K_2O- and Al_2O_3-poor, relatively Fe-rich grunerite–garnet rocks.

As was demonstrated by Korikovsky (1979), a low K_2O concentrations in metapelites is, at certain temperatures and pressures, an important extensive factor of equilibrium, and no composition dependence of the stability of any mineral can be determined irrespective of its assemblage. For instance, the *P–T* parameters of hypersthene stability significantly vary depending on other minerals coexisting with it in assemblages, whether these are potassic feldspar, cummingtonite, gedrite, or anthophyllite and whether quartz is present or not. By way of illustration, the onset of orthopyroxene crystallization in quartz-free metamorphosed ultramafic rocks depends on P_{CO_2}, and this mineral can appear at temperatures as low as 500–600°C (Will *et al.*, 1990).

METAMORPHIC ZONING

The K_2O-rich metapelites of the Prioskol'skaya area were determined to have metamorphic zoning of the andalusite–sillimanite type, in which the staurolite decomposition isograde was mapped between the staurolite–sillimanite and sillimanite–muscovite zones (Fig. 2). No mineral assemblages of the potassic feldspar–cordierite zone were reliably identified. Available petrographic data make it possible to distinguish two temperature grades of the sillimanite–muscovite zone: sillimanite–muscovite and higher temperature sillimanite–muscovite–potassic feldspar, which can be recognized by the appearance of potassic feldspar in muscovite-bearing rocks.

Metapelites of the staurolite–sillimanite zone are relatively rare and were mapped in the central portion of the structure. The most widespread rocks of the Prioskol'skya structure are crystalline schists of the sillimanite–muscovite zone (Fig. 2).

The critical mineral assemblages of these rocks are *St + Sil + Bt + Qtz + Pl + Grt* for the staurolite–muscovite zone, *Qtz + Pl + Ms + Bt + Grt + Sil* for the muscovite–sillimanite zone, and *Sil + And + Ms + Grt + Bt + Spl + Kfs* for the quartz-free rocks (Table 1).

The isograde of staurolite decomposition in the K-poorer but Fe-richer rocks coincides with the analogous isograde in K-rich metapelites. The more magnesian rocks with the $Ged_{44} + Ath_{46} + Crd_{34} + Bt$ assemblage contain no staurolite, because this mineral in all of our rocks is more ferrous. The appearance of orthopyroxene in assemblage with gedrite and garnet (Sample 5257/23.2) marks the hypersthene–gedrite–garnet metamorphic grade, which corresponds to the high-temperature part of the muscovite–sillimanite zone.

Table 1. Mineral assemblages of K_2O-rich metapelites of the Prioskol'skaya area

Sample	*Qtz*	*Pl*	*Bt*	*St*	*Crd*	*Grt*	*Sil*	*And*	*Ol*	*Ms*	*Kfs*	*Ged*	*Opx*	*Ath*	*Gru*	*Mag*	*Spl*
	K_2O-rich metapelites																
Staurolite–sillimanite zone																	
5264/228	+	+	+	+	–	+	+	–	–	+	–	–	–	–	–	–	–
Muscovite–sillimanite zone																	
low-temperature grade																	
5257/20	–	–	+	–	–	+	+	+	–	+	+	–	–	–	–	–	+
5429/297	+	–	+	–	–	–	+	–	–	+	–	–	–	–	–	+	–
5420/6	+	+	+	–	–	–	+	+	–	+	–	–	–	–	–	+	–
high-temperature grade																	
5267/11	+	–	+	–	–	–	–	–	–	+	+	–	–	–	–	+	–
5267/13	+	+	+	–	–	–	–	–	–	+	+	–	–	–	–	–	–
185-A/15	+	–	+	–	–	–	–	–	–	+	+	–	–	–	–	–	–
5259/531	+	–	+	–	–	–	–	–	–	+	+	–	–	–	–	–	–
5256/244	+	+	+	–	–	+	–	–	–	–	–	–	–	–	–	+	–
5481/12	+	–	+	–	–	–	–	–	–	–	+	–	–	–	–	+	–
5481/3	+	–	+	–	–	–	+	–	–	–	–	–	–	–	–	+	–
5274/8	+	–	+	–	+	–	+	–	–	–	–	–	–	–	–	+	–
	K_2O-poor metapelites																
Staurolite–sillimanite zone																	
5264/212	+	+	+	+	+	–	–	–	–	–	–	–	–	–	–	+	–
Muscovite–sillimanite zone																	
5257/23.2	–	–	+	–	–	+	–	–	–	–	–	+	+	–	–	+	–
5257/23.1	–	–	–	–	+	–	–	–	–	–	–	+	–	+	–	+	–
5257/22	+	–	–	–	+	+	+	–	–	–	–	+	–	+	–	+	–
5420/2	–	–	–	–	+	+	–	–	–	–	–	+	–	+	–	+	–
5267/290	–	–	–	–	–	+	–	–	+	–	–	+	+	–	–	+	+
5422/16	+	–	–	–	–	–	–	–	–	–	–	–	–	–	+	+	–
5262/100	–	+	+	–	–	–	–	–	–	–	–	–	–	–	+	+	–
5422/16	–	–	+	–	–	+	–	–	–	–	–	–	–	–	+	+	–
5429/344	–	+	+	–	–	–	–	–	–	–	–	–	–	–	+	+	–

METHODS

All of our metapelite samples are fragments of the core from holes, which was thoroughly described during fieldworks. The samples were examined optically, and their minerals were analyzed on a Camebax SX-50 microprobe at the Moscow State University at an accelerating voltage of 15 kV, beam current of 1–2 nA, and beam diameter of 1–2 μm. The accuracy of the analyses was systematically controlled with the use of natural and synthetic standards. The crystal chemical formulas of minerals were normalized to the following numbers of oxygen atoms: 4 for olivine and spinel, 5 for sillimanite, 6 for orthopyroxene, 8 for feldspars, 11 for biotite, 12 for garnet, 18 for cordierite, 23 for amphiboles, and 46 for staurolite. The *P–T* parameters of metamorphism were calculated by the TPF computer program (Fonarev *et al.*, 1991). Back-scattered electron images of thin sections were taken on a CamScan electron microscope with a Link ED system at the Moscow State University.

MINERALOGY

We thoroughly examined, using a microprobe, the chemistry and zoning of minerals in gedrite–anthophyllite and grunerite–garnet schists (Samples 5264/212, 5257/23.1, 5257/23.2; 5262/100, 5422/16, and 5267/290) and K_2O-rich metapelites (Samples 5264/228 and 5257/20).

The mineral assemblages of rocks from the Prioskol'skaya area are listed in Table 1, and analyses of the minerals are summarized in Tables 2–10.

K_2O-Poor Rocks

Depending on their X_{Fe} and X_{Al}, the K_2O-poor schists contain the assemblages *Gru + Bt + Grt + Mag + Qtz + Pl* (in relatively Fe-rich varieties) and *Ath + Ged + Bt + Crd + Mag ± Grt ± Opx ± Qtz* (in more magnesian and aluminous varieties). Sample 5267/290 was determined to contain the unusual assemblage *Ol + Ged + Grt + Opx + Mag*. This sample represents a quartz-free, K_2O-poor rock (Figs. 3a, 3b). We had no analyses of rocks with this assemblage, but judging from the absence of cordierite and the abundance of garnet and magnetite, the rock is a Fe-richer quartz-free equivalent of anthophyllite–gedrite–cordierite schists.

Fe–Mg amphiboles of the relatively magnesian and aluminous metapelites are anthophyllite (Figs. 3c, 3d) and gedrite. The Prioskol'skaya metapelites widely contain the assemblage of gedrite and anthophyllite with cordierite. The gedrite and anthophyllite occur as prismatic crystals with sharp linear contacts. In accordance with the amphibole nomenclature (Leake *et al.*, 1997), anthophyllite contains up to 8 wt % Al_2O_3 and 7.0–8.0 f.u. Si, while gedrite has >8 wt % Al_2O_3 and 6.0–7.0 f.u. Si. These relations are illustrated in Fig. 4. As is known, the gedrite–anthophyllite isomorphous series has a miscibility gap, at least if the temperature is no higher than 600–610°C (Spear, 1980; Robinson *et al.*, 1982).

The anthophyllite develops as colorless and brownish gray elongated platy crystals up to 4–6 mm with the lowest X_{Fe} among the amphiboles (40.8–43.5 at. %) and contain 3–6 wt % Al_2O_3 (Table 2).

The gedrite forms tabular crystals up to 2–3 mm with, a clear pleochroism from grayish blue to brownish gray. The mineral is usually associated with anthophyllite, except Sample 5257/23.2, in which gedrite coexists with orthopyroxene but not anthophyllite (Sample 3d), and Sample 5267/90), in which this mineral is accompanied by olivine, orthopyroxene, and garnet (Figs. 3a, 3b).

The X_{Fe} of the gedrite is higher than that of the anthophyllite and ranges from 46.3 to 48.8 at. % (Table 2). The X_{Fe} of the gedrite in association with orthopyroxene and olivine (Sample 5267/290) is 40.3–49.1 at. %, which is higher that the X_{Fe} of the coexisting orthopyroxene but lower than this parameter of the olivine. The composition of gedrite from anthophyllite–gedrite–cordierite schist in the Priaskol'skaya area displays broad variations in terms of Al_2O_3 concentrations, from 9.3 to 16.2 wt % (Table 2). The gedrite in association with olivine, orthopyroxene, and garnet is higher in alumina (15.6–17.3 wt % Al_2O_3), which is close to the limiting value for this mineral (Table 2). The presence of 0.30–0.75 f.u. Na makes the gedrite close to the idealized formula $Na_{0.5}(Mg, Fe)_{5.5}Al_{1.5}[Si_6Al_2O_{22}](OH)_2$ (Robinson *et al.*, 1971).

The grunerite occurs as large (up to 1 cm) prismatic crystals, often with polysynthetic twinning in the Fe-rich rocks, in which it is present in association with quartz, garnet, biotite, and plagioclase but never in assemblage with anthophyllite, gedrite, or cordierite. The X_{Fe} of the grunerite equals 63.2–68.8 at. % in assemblage with garnet (Sample 5422/16) and rises even higher, 78.9–79.0 at. %, in the plagioclase–grunerite rocks. The grunerite contains minor amounts of Al_2O_3 (0.49–0.74 wt %), MnO (0.14–0.55 at. %), and CaO (0.43–0.63 at. %) (Table 2).

Cordierite is present in our samples in association with orthoamphiboles (Samples 5257/23.1 and 5257/22). This minerals occurs as rounded or irregularly shaped grains or short-prismatic crystals up to 1.25 mm (Fig. 3c). The X_{Fe} of this mineral is 22–23% in Samples 5257/23.1 and 29.3–34.0 in Sample 5257/22 (Table 3). The cordierite is relatively high in Na_2O, from 0.07 to 0.75 wt %.

Cordierite rims around staurolite crystals in the staurolite–sillimanite zone were encountered only in Sample 5264/212 (Fig. 3e). This mineral is moderately magnesian (X_{Fe} = 36.2–37.8) and contains an admixture of Na_2O (0.29–0.45 wt %) (Table 3).

Staurolite was detected only in the form of small crystals armored by cordierite rims (Sample 5264/212; Fig. 3e), whose cores have X_{Fe} = 85.0–86.4 and rims

Table 2. Representative analyses (wt %) of amphiboles from metapelites of the Prioskol'skaya area

Component	5257/23.1				5257/22							
	Ged-10	*Ath*-11	*Ath*-18	*Ath*-16	*Ath*-1	*Ath*-2	*Ath*-3	*Ath*-4	*Ath*-5	*Ath*-6	*Ged*-11	*Ath*-12
		core	core	margin	core	margin	core	margin	core	margin	core	margin
SiO_2	44.50	57.23	52.90	51.30	53.80	53.57	54.92	52.92	51.46	53.28	48.12	52.35
TiO_2	0.17	0.05	0.08	0.82	0.06	0.05	0.07	0.05	0.07	0.03	0.12	0.06
Al_2O_3	14.73	5.49	4.54	5.67	3.03	2.99	3.07	3.88	6.06	3.17	9.33	3.65
Cr_2O_3	0.44	0.32	0.23	0.40	–	0.10	0.05	–	–	–	0.29	0.01
FeO	20.84	18.84	21.80	21.24	23.30	23.12	22.41	22.34	22.84	22.90	23.45	22.73
MnO	0.16	0.21	0.21	0.14	0.14	0.19	0.17	0.19	0.17	0.17	0.27	0.22
MgO	13.57	17.11	17.80	16.73	17.70	17.13	17.11	17.68	17.42	16.71	14.67	17.52
CaO	0.46	0.38	0.34	0.33	0.20	0.18	0.21	0.14	0.27	0.21	0.26	0.21
ClO	0.01	–	–	–	0.15	0.04	0.27	0.11	–	–	0.05	–
ZnO	0.16	–	–	0.15	0.02	0.04	0.03	0.02	0.07	0.13	0.70	0.15
Na_2O	1.45	0.45	0.39	0.47	0.22	0.25	0.21	0.29	0.49	0.31	1.57	0.39
K_2O	–	0.03	0.01	–	0.01	0.01	0.01	0.01	0.03	0.05	0.07	0.02
Total	96.49	96.59	98.30	97.25	98.90	97.70	98.55	97.63	98.24	97.62	98.90	97.32
						23O						
Si	6.71	7.61	7.61	7.52	7.73	7.77	7.87	7.68	7.46	7.76	7.06	7.66
Ti	0.02	0.02	0.01	0.01	0.01	0.01	0.01	0.01	0.01	–	0.01	0.01
Al(VI)	1.46	0.06	0.39	0.51	0.24	0.20	0.11	0.32	0.62	0.19	1.00	0.36
Al(IV)	1.09	0.84	0.38	0.47	0.28	0.31	0.41	0.35	0.40	0.35	0.60	0.27
Cr	0.05	0.03	0.03	0.05	–	0.01	0.01	–	–	–	0.03	–
Fe^{3+}	0.44	0.27	0.06	0.01	0.01	0.05	0.19	0.03	0.21	0.07	0.50	0.11
Fe^{2+}	2.11	1.91	2.56	2.58	2.80	2.77	2.49	2.68	2.52	2.73	2.35	2.66
Mn	0.02	0.03	0.03	0.02	0.02	0.02	0.02	0.02	0.02	0.02	0.03	0.03
Mg	2.92	3.60	3.81	3.66	3.80	3.73	3.66	3.82	3.61	3.78	3.21	3.82
Ca	0.07	0.06	0.05	0.05	0.03	0.03	0.03	0.02	0.04	0.03	0.04	0.03
Zn	0.02	–	–	0.02	0.02	–	0.03	0.01	–	–	0.01	–
Cl	–	–	–	–	0.01	0.01	0.01	0.01	0.02	0.03	0.17	0.04
Na	0.32	0.12	0.11	0.14	0.06	0.07	0.06	0.08	0.14	0.09	0.45	0.11
K	–	–	–	–	–	–	–	–	0.01	0.01	0.01	–
X_{Fe}	0.46	0.41	0.41	0.42	0.42	0.43	0.42	0.41	0.44	0.42	0.47	0.42

Table 2. (Contd.)

Component	5257/23.2		5422/16			5262/100		5267/290		
	Ged-45	*Ged*-46	*Gru*-21	*Gru*-22	*Gru*-24	*Gru*-54	*Gru*-55	*Ged*-45	*Ged*-3	*Ged*-7
	margin, near *Grt*	core	margin, near *Grt*	core	matrix	core	margin			
SiO_2	44.83	43.70	51.37	51.14	50.73	49.62	49.64	43.86	43.77	49.13
TiO_2	0.16	0.15	0.03	–	–	0.03	0.03	0.03	–	0.02
Al_2O_3	15.44	16.20	0.49	0.49	0.54	0.74	0.55	17.26	15.59	5.39
Gr_2O_3	0.21	0.09	–	0.08	0.24	–	0.05	0.04	–	0.02
FeO	22.38	22.21	34.09	35.42	35.44	42.11	42.67	19.32	20.67	26.25
MnO	0.29	0.31	0.49	0.55	0.36	0.30	0.14	0.25	0.22	0.36
MgO	14.35	14.27	11.13	9.02	9.01	6.30	6.35	16.07	16.69	18.52
CaO	0.65	0.66	0.44	0.43	0.44	0.63	0.44	0.44	0.31	0.17
ClO	0.01	–	0.02	0.19	–	0.04	–	0.09	–	0.02
ZnO	0.07	0.02	0.05	0.01	0.03	–	0.02	–	–	0.08
Na_2O	1.61	1.64	0.06	0.06	0.09	0.15	0.09	2.55	2.75	0.04
K_2O	0.01	–	0.01	0.02	0.02	–	0.02	0.01	0.01	–
Total	100.00	99.24	98.18	97.41	96.90	100.00	100.00	99.93	100.00	100.00
					23O					
Si	6.44	6.33	7.98	7.98	7.96	7.80	7.81	6.24	6.28	7.16
Ti	0.02	0.02	–	–	–	–	–	–	–	–
Al(VI)	1.63	1.73	0.02	0.02	0.04	0.16	0.14	1.04	0.78	0.79
Al(IV)	0.96	1.00	0.08	0.07	0.06	–	–	1.83	1.81	0.14
Cr	0.03	0.01	–	–	–	–	0.01			–
Fe^{3+}	0.58	0.56	0.00	0.02	0.02	0.00	0.00	0.53	0.68	0.24
Fe^{2+}	2.08	2.11	4.18	4.60	4.62	5.56	5.65	1.73	1.76	2.98
Mn	0.04	0.04	0.06	0.07	0.05	0.04	0.02	0.03	0.03	0.04
Mg	3.07	3.08	2.55	2.10	2.11	1.48	1.49	3.41	3.57	4.02
Ca	0.10	0.10	0.07	0.07	0.07	0.11	0.07	0.07	0.05	0.03
Zn	0.01	–	–	0.02	–	–	–	–	–	–
Cl	–	–	–	–	–	0.01	–	0.02	–	–
Na	0.45	0.46	0.02	0.02	–	0.04	0.03	0.70	0.75	0.01
K	–	–	–	0.01	–	–	–	–	–	–
X_{Fe}	0.47	0.47	0.63	0.69	0.70	0.79	0.79	0.40	0.49	0.44

Note: Here and in Tables 3–10, dashes mean concentrations below the analytical determination threshold.

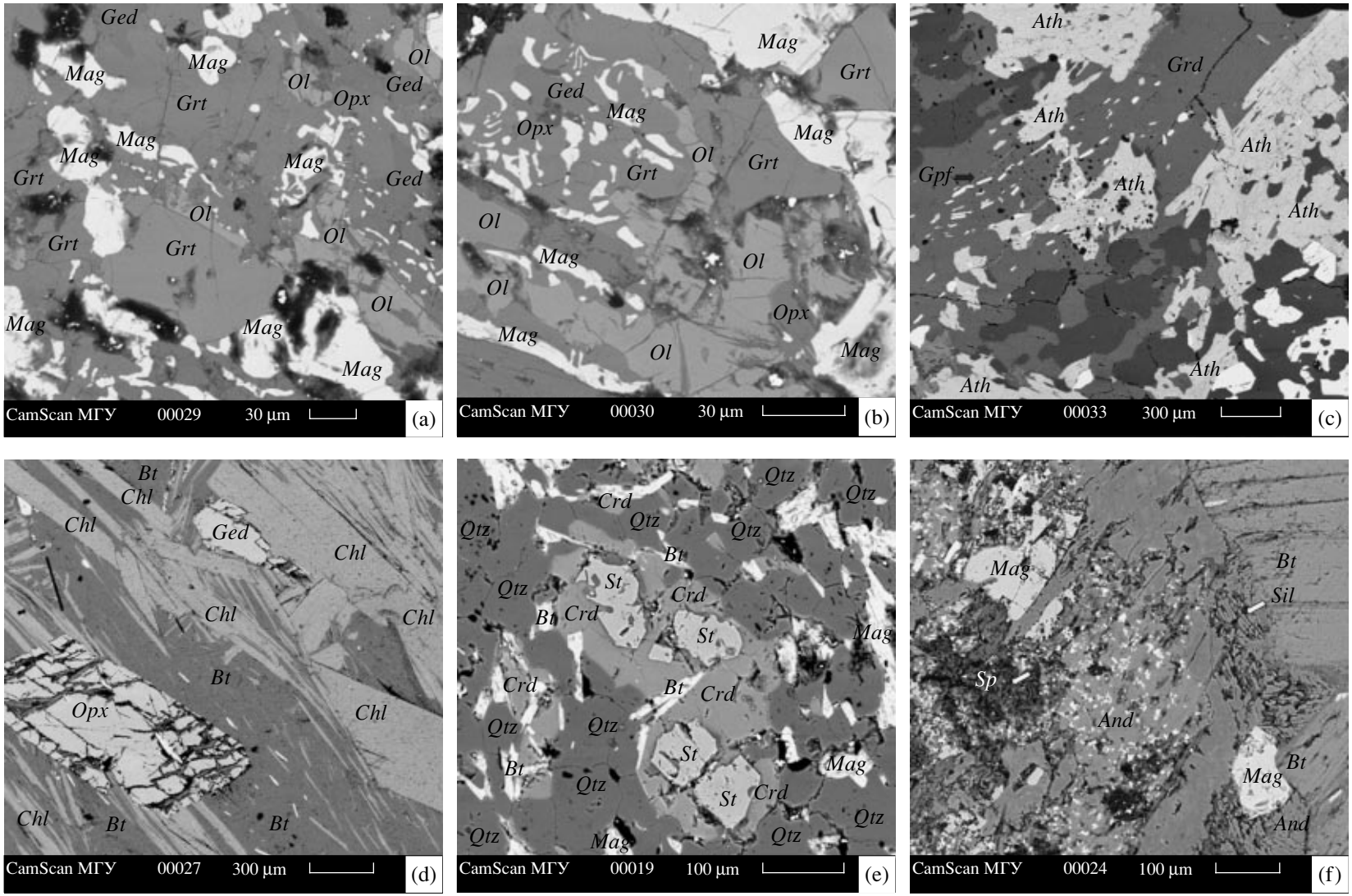

Fig. 3. BSE images of reaction textures in rocks of the Prioskol'skaya area.

(a) Garnet + olivine + orthopyroxene + gedrite assemblage (Sample 5267/290). (b) "Emulsion" magnetite inclusions in silicates (Sample 5267/290). (c) Orthoamphibole + cordierite assemblage (Sample 5257/20). (d) Gedrite + orthopyroxene assemblage (Sample 5257/23.2). (e) Cordierite rims around staurolite (Sample 5264/212). (f) Spinel inclusions in andalusite and andalusite replacement by sillimanite (Sample 5257/20).

Table 3. Representative analyses (wt %) of cordierite from metapelites of the Prioskol'skaya area

Component	5257/23.1	5257/22				5264/212			
	Crd-13	*Crd*-7	*Crd*-8	*Crd*-9	*Crd*-10	*Crd*-25	*Crd*-26	*Crd*-28	*Crd*-35
	margin	core	margin	core	margin	*Crd* rims around *St*			
SiO_2	50.22	47.07	47.41	49.34	49.30	47.06	47.28	46.98	48.04
TiO_2	–	–	0.01	–	0.02	0.02	–	–	–
Al_2O_3	34.18	29.04	30.32	30.48	31.12	33.44	32.74	36.52	33.77
Cr_2O_3	–	–	0.05	–	–	0.01	0.04	0.05	0.14
FeO	5.09	9.93	8.72	7.64	6.75	8.39	8.36	10.60	8.11
MnO	0.08	0.05	–	0.03	0.06	0.02	0.13	0.15	0.09
MgO	9.85	10.80	10.46	9.08	9.14	7.73	7.86	5.37	7.99
CaO	0.10	1.52	1.45	1.74	1.09	0.02	0.05	0.53	0.03
ClO	–	0.10	0.08	0.12	0.53	0.08	0.03	0.11	0.04
ZnO	–	–	0.15	–	–	0.04	0.01	–	–
Na_2O	0.24	0.07	0.11	0.16	0.75	0.45	0.37	0.29	0.44
K_2O	0.08	0.93	1.10	1.14	1.02	0.02	0.02	0.31	0.01
Total	99.84	99.50	99.82	99.72	99.88	97.29	96.91	100.00	98.67
				18O					
Si	5.01	4.90	4.91	5.05	5.04	4.91	4.95	4.83	4.94
Ti	–	–	–	–	–	–	–	–	–
Al	4.02	3.62	3.71	3.71	3.78	4.12	4.04	4.32	4.09
Cr	–	–	–	–	–	–	–	–	0.01
Fe^{2+}	0.43	0.86	0.76	0.65	0.58	0.73	0.73	0.91	0.70
Mn	0.01	–	–	–	0.01	–	0.01	0.01	0.01
Mg	1.47	1.68	1.61	1.39	1.39	1.20	1.23	0.82	1.23
Ca	0.01	0.17	0.16	0.19	0.12	–	0.01	0.06	–
Zn	–	–	0.01	–	–	0.01	–	–	–
Cl	–	0.02	0.01	0.02	0.09	0.01	–	0.02	0.01
Na	0.05	0.01	0.02	0.03	0.15	0.09	0.08	0.06	0.09
K	0.01	0.12	0.12	0.15	0.14	–	–	0.04	–
X_{Fe}	0.23	0.34	0.32	0.32	0.29	0.38	0.37	0.54	0.36

have X_{Fe} = 84.1–84.2 (Table 10). It is worth noting the low ZnO concentration (0.08–0.38 wt %) in staurolite from Sample 5264/212, although the high-temperature staurolite (in assemblage with sillimanite) may contain as much as 2 wt % ZnO.

Olivine was detected in Sample 5267/290 in association with orthopyroxene, gedrite, and garnet, in which it occurs in the groundmass as irregularly-shaped elongated grains up to 1 mm long (Figs. 3a, 3b). The olivine occurs in physical contact with all minerals of this rock and compositionally corresponds to hyalosiderite. The groundmass olivine has X_{Fe} of 51.6–54.2, and its grains in contact with garnet are a little bit more ferrous, 55.2–55.6 at. % (Table 4). The admixtures are MnO (0.18–0.30 wt %) and Na_2O (0.03–0.16 wt %).

Orthopyroxene was found only in Samples 5257/23.2 and 5267/290, in which it is contained in the form of small grains in association with gedrite and garnet (Sample 5257/23.2, Fig. 3d) or with olivine, gedrite, garnet, and magnetite (Sample 5267/290, Figs. 3a, 3b). The orthopyroxene is low in Fe (X_{Fe} = 33.6–44.3) and contains 2 wt % Al_2O_3 (Table 5). The orthopyroxene from Sample 5267/290 forms crystals of variable sizes, from 0.5 to 2.0 mm (Figs. 3a, 3b) and inclusions in garnet and contains 0.54–2.72 wt % Al_2O_3, with the least aluminous orthopyroxene occurring as inclusions in garnet (0.79–0.87 wt % Al_2O_3) and small crystals (up to 0.54 wt % Al_2O_3). The orthopyroxene of both assemblages (*Qtz* + *Bt* + *Grt* + *Opx* and *Ol* + *Opx* + *Grt* + *Ged* + *Mag*) has very close compositions.

Table 4. Representative analyses (wt %) of olivine from metapelites of the Prioskol'skaya area

Component	5267/290					
	Ol-48	*Ol*-9	*Ol*-4	*Ol*-11	in contact with *Grt*	
					Ol-12	*Ol*-9
SiO_2	35.49	34.20	33.42	33.20	33.31	33.31
TiO_2	0.02	–	0.02	–	0.03	–
Al_2O_3	0.01	0.01	–	0.02	–	–
FeO	42.70	44.08	44.48	44.94	45.56	45.87
MnO	0.30	0.18	0.23	0.35	0.30	0.25
MgO	21.15	21.48	21.60	21.27	20.77	20.58
CaO	0.01	–	0.06	0.09	0.03	–
Na_2O	0.14	0.03	0.16	0.12	–	–
K_2O	0.05	–	0.04	0.02	0.01	–
Total	100.00	100.00	100.00	100.00	100.00	100.00
			4O			
Si	1.02	1.00	0.98	0.98	0.98	0.98
Ti	–	–	–	–	–	–
Al	–	–	–	–	–	–
Fe	1.03	1.07	1.09	1.10	1.12	1.13
Mn	0.01	0.01	0.01	0.01	0.01	0.01
Mg	0.91	0.93	0.94	0.93	0.91	0.90
Ca	–	–	–	–	–	–
Na	0.01	–	0.01	0.01	–	–
K	–	–	–	–	–	–
X_{Fe}	0.53	0.54	0.54	0.54	0.55	0.56

Garnet is present in approximately every third sample as large subhedral crystals of dodecahedral habit, from 1 to 6 mm across. When in assemblage with orthoamphibole, cordierite, and orthopyroxene, the garnet is fairly magnesian: X_{Fe} = 65.0–72.3 (Sample 5257/23.2), 77.1–79.5 (Sample 5257/22), and 69.3–74.1 (Sample 5267/290 (Table 6). Garnet crystals are compositionally zoned, with X_{Mg} decreasing and, correspondingly, X_{Fe} increasing from the cores to margins, irrespective of other minerals occurring in contact with the garnet grains. In a large garnet grain from Sample 5257/23.2, the X_{Ca} weakly increases toward the margins, while the increase in the X_{Mn} is more significant (Fig. 5a). Conversely, the garnet from Sample 5257/22 is characterized by a marginward increase in X_{Ca} but no changes in X_{Mn}.

The garnet of Sample 5267/290 composes 2-mm subhedral crystals, which are either homogeneous or abound in irregularly shaped and vermicular inclusions ("emulsion," Figs. 3a, 3b). This garnet is relatively magnesian, X_{Mg} = 25.9–30.7 at. % (Table 6), with 0.25–0.29 pyrope and 0.66–0.70 almandine end members. The concentrations of the grossular and spessartine components are insignificant, and their sums do not exceed 0.05. The garnet shows no pronounced zoning.

The composition of garnet in the *Ol–Ged–Grt–Opx–Mag* assemblage is generally close to the composition of this mineral in gedrite–anthophyllite–cordierite schists, which are widespread within the Prioskol'skaya area.

In the relatively Fe-rich rocks, garnet is in association with grunerite and occurs as dodecahedral crystals,

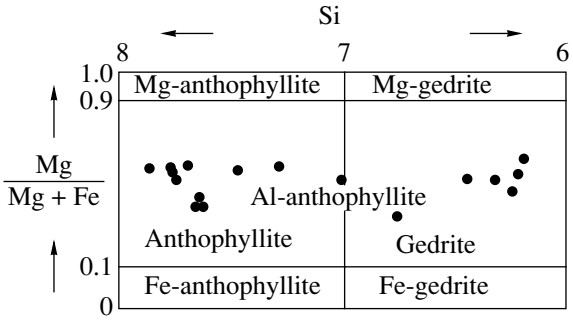

Fig. 4. Mg/(Mg + Fe) vs. Si (f.u.) diagram for anthophyllite and gedrite in metapelite of the Prioskol'skaya area.

Table 5. Representative analyses (wt %) of orthopyroxene from metapelites of the Prioskol'skaya area

Component	5267/290				5257/23.2
	Opx-2	*Opx*-3	*Opx*-51	*Opx*-14	*Opx*-47
SiO_2	55.51	53.46	52.16	51.89	54.19
TiO_2	0.07	0.04	–	0.02	0.04
Al_2O_3	1.44	1.19	1.05	0.79	2.01
Cr_2O_3	–	0.06	0.13	–	0.06
FeO	20.80	24.68	25.01	25.86	23.01
MnO	0.17	0.15	0.11	0.22	0.35
MgO	21.56	21.14	21.12	21.17	19.93
CaO	0.16	0.07	0.14	0.04	0.33
ClO	–	0.01	–	–	0.05
ZnO	–	–	–	–	0.01
Na_2O	0.29	0.01	0.05	–	0.17
K_2O	–	–	0.02	–	0.01
Total	100.00	100.80	99.79	100.00	100.14
			6O		
Si	2.03	1.99	1.97	1.96	2.02
Ti	0.00	–	–	–	–
Al	0.06	0.05	0.05	0.04	0.09
Cr	–	–	–	–	–
Fe	0.64	0.77	0.79	0.82	0.71
Mn	0.01	0.01	–	0.01	0.01
Mg	1.18	1.17	1.189	1.19	1.09
Ca	0.01	–	0.01	–	0.01
Zn	–	–	–	–	–
Cl	–	–	–	–	–
Na	0.02	–	0.04	–	0.01
K	–	–	–	–	–
X_{Fe}	0.35	0.40	0.40	0.41	0.39
Fs	0.35	0.40	0.40	0.41	0.39
En	0.65	0.60	0.60	0.59	0.60
Wo	–	–	–	–	0.01

up to 3 mm across, with numerous quartz inclusions. The cores of garnet grains abound in inclusions, while their peripheral parts are homogeneous. The garnet composition corresponds to almandine (X_{Fe} = 92.3–95.2). The zoning differs from that in garnet from the magnesian metapelites: the Mg and Ca concentrations increase from cores to margins that are in contact with biotite and grunerite, whereas the Mn concentrations simultaneously decrease. The Fe distribution reveals no zoning (Fig. 5b).

Biotite is contained in both the magnesian and ferrous varieties of K_2O-poor metapelites. The mineral is present in the rock matrices and as inclusions in garnet (Sample 5257/23.2). The biotite in association with grunerite (Sample 5422/16) is quite high in Fe (X_{Fe} = 68.3–70.7 at. %) and, conversely, fairly magnesian (X_{Fe} = 34.0–35.8 at. %) in association with gedrite (Sample 5257/23.2; Table 7). In both rock types, biotite is low in titania (1.02–1.24 wt % TiO_2).

Plagioclase is a rare mineral in the gedrite–anthophyllite rocks. It was found in association with grunerite in Sample 5262/100. Chemically, it is almost homogeneous (unzoned) oligoclase ($Ab_{85.9–86.0}An_{14.0–14.1}$) or slightly more sodic ($Ab_{93.2–95.5}An_{4.5–6.8}$) in Sample 5264/212 (Table 8).

Magnetite is present in practically all samples of the K_2O-poor rocks. Magnetite in Sample 5267/290 develops as anhedral crystals up to 2–2.5 mm across in

Table 6. Representative analyses (wt %) of garnet from metapelites of the Prioskol'skaya area

Component	5422/16			5257/20		5264/228		5257/22		5257/23.2			5267/290			
	Grt-9	*Grt*-15	*Grt*-17	*Grt*-18	*Grt*-19	*Grt*-1	*Grt*-2	*Grt*-5	*Grt*-8	*Grt*-31	*Grt*-12	*Grt*-38	*Grt*-32	*Grt*-50	*Grt*-2	*Grt*-11
	margin	core	margin	core	margin	core	margin		margin	core	margin	core				
	Bt		*Gru*		*Bt*		*Bt*		*Ath*		*Bt*	*Bt*				
SiO_2	35.94	35.32	35.42	37.50	37.40	36.25	36.78	37.13	36.89	37.69	37.06	37.15	38.76	38.86	37.96	37.27
TiO_2	–	0.02	–	0.04	–	–	–	–	0.02	0.02	0.03	0.01	–	0.07	–	–
Al_2O_3	21.41	21.24	21.53	22.09	22.53	21.89	21.65	22.55	22.20	22.16	22.97	22.18	21.59	22.52	21.50	21.51
Cr_2O_3	–	–	–	–	–	–	–	–	–	–	–	–	–	0.08	0.07	–
FeO	35.52	36.57	35.64	32.17	30.28	37.32	38.07	31.48	32.61	29.64	30.70	30.65	30.78	29.60	31.97	32.08
MnO	2.35	3.67	2.51	1.86	2.37	0.45	0.36	0.98	0.98	0.92	1.48	1.69	0.83	0.84	0.73	0.99
MgO	1.39	0.89	1.42	4.99	5.15	3.78	3.39	5.25	4.71	6.61	5.07	5.30	7.66	6.72	6.28	6.77
CaO	3.80	2.05	3.77	1.88	2.63	0.29	0.21	2.02	1.95	2.42	2.68	2.62	1.21	1.26	1.44	1.19
Total	100.4	99.76	100.3	100.5	100.4	99.98	99.95	99.42	99.36	99.47	100.0	99.59	100.88	100.00	100.00	100.00
								12O								
Si	2.92	2.92	2.89	2.97	2.93	2.98	2.99	2.95	2.95	2.96	2.92	2.95	3.00	3.02	2.99	2.95
Ti	–	–	–	–	–	–	–	–	–	–	–	–	–	–	–	–
Al	2.05	2.07	2.08	2.05	2.08	2.08	2.08	2.11	2.09	2.05	2.14	2.07	1.97	2.06	2.00	2.01
Cr	–	–	–	–	–	–	–	–	–	–	–	–	–	0.01	0.01	–
Fe	2.42	2.52	2.42	2.12	1.99	2.44	2.46	2.09	2.18	1.95	2.03	2.03	1.99	1.92	2.11	2.12
Mn	0.16	0.26	0.17	0.12	0.16	0.03	0.02	0.07	0.07	0.06	0.10	0.11	0.05	0.05	0.05	0.07
Mg	0.17	0.11	0.18	0.59	0.65	0.42	0.40	0.62	0.56	0.77	0.60	0.63	0.88	0.78	0.74	0.80
Ca	0.33	0.18	0.34	0.16	0.22	0.02	0.02	0.17	0.17	0.20	0.23	0.22	0.10	0.10	0.12	0.11
Alm	0.79	0.82	0.78	0.71	0.66	0.84	0.85	0.71	0.73	0.65	0.69	0.68	0.66	0.67	0.70	0.69
Sps	0.05	0.08	0.06	0.04	0.05	0.01	0.01	0.02	0.02	0.02	0.03	0.04	0.02	0.02	0.02	0.02
Prp	0.06	0.04	0.06	0.20	0.21	0.15	0.14	0.21	0.19	0.26	0.20	0.21	0.29	0.27	0.25	0.26
Grs	0.11	0.06	0.11	0.05	0.07	0.01	–	0.06	0.06	0.07	0.78	0.07	0.03	0.03	0.04	0.03
X_{Fe}	0.93	0.95	0.93	0.74	0.76	0.85	0.86	0.77	0.79	0.71	0.77	0.76	0.69	0.71	0.74	0.73

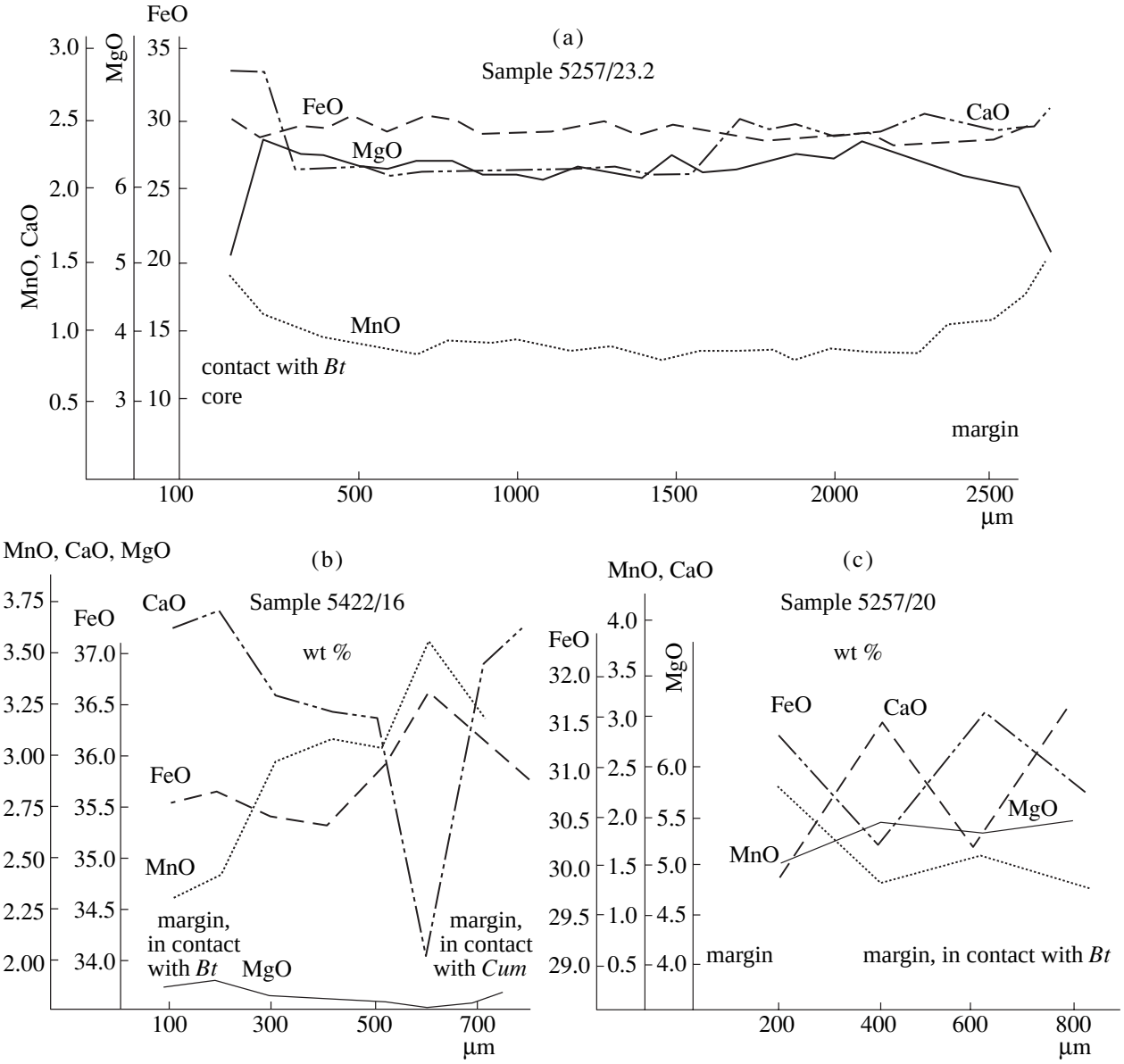

Fig. 5. Types of garnet zoning in metapelites of the Prioskol'skaya area.

amounts of 5–7 modal % and also occurs as vermicular "emulsion" in garnet (Fig. 3b). Its composition corresponds to virtually pure magnetite with minor amounts of TiO_2, Al_2O_3, MnO, MgO, and Cr_2O_3 (Table 9). The mineral contains small spinel inclusions.

Secondary talc was encountered in Sample 5267/290 in association with olivine, orthopyroxene, gedrite, and garnet. The diaphthoritic talc develops as aggregates of small platy or flaky crystals replacing olivine. The talc exhibits broad variations in its X_{Fe}, from 18.4 to 46.7% (Table 9).

Spinel was detected in the K_2O-poor metapelites only in Sample 5267/290, in which it occurs in assemblage with magnetite. The spinel of the olivine-bearing metapelites was identified only as inclusions in magnetite crystals. These are small anhedral grains of brown color, with X_{Fe} = 68.9–92.1%, compositionally corresponding to hercynite (Table 9). The mineral is an exsolution product of the magnetite solid solution.

K_2O-Rich Metapelites

Staurolite occurs as small (no larger than 0.5 mm) anhedral or elongated grains. The X_{Fe} of staurolite in association with garnet and sillimanite ranges over the narrow interval of 83.4–84.6 without any systematic variations over individual grains (Table 10).

Garnet is contained in the metapelites of the staurolite–sillimanite zone (Sample 5264/228) in the form of equant, inclusion-free dodecahedral grains up to 2 mm

Table 7. Representative analyses (wt %) of biotite and chlorite from metapelites of the Prioskol'skaya area

Component	5422/16			5257/20		5264/228			5420/6		
	Bt-19	*Bt*-20	*Bt*-23	*Bt*-25	*Bt*-26	*Bt*-2	*Bt*-4	*Bt*-9	*Bt*-49	*Bt*-50	*Bt*-53
	margin	core	matrix	margin	core	margin	margin	core			
	Grt			*Grt*		*Grt*					
SiO_2	34.69	34.60	34.16	37.94	37.22	34.91	35.69	35.38	38.51	38.78	38.69
TiO_2	1.21	1.18	1.02	1.27	1.83	1.60	1.64	1.63	0.37	0.64	0.78
Al_2O_3	16.40	15.70	15.94	17.92	17.68	18.37	18.19	19.25	21.77	21.70	21.27
Cr_2O_3	0.07	0.27	0.86	0.15	0.57	0.69	0.09	0.25	–	–	–
FeO	26.07	27.00	26.11	13.77	15.80	18.65	18.07	17.72	15.83	15.12	15.25
MnO	0.13	0.07	0.59	0.02	0.02	0.07	0.03	0.04	0.14	0.07	0.25
MgO	6.78	6.46	6.19	14.53	14.66	10.94	11.23	10.82	13.40	13.57	13.31
CaO	0.01	0.08	0.33	0.06	0.11	0.27	0.03	0.06	–	0.01	0.02
ZnO	–	0.22	0.03	0.07	0.14	0.06	0.07	0.14	–	–	–
ClO	0.48	0.53	0.61	–	–	0.49	–	0.11	0.08	0.12	0.06
Na_2O	0.13	0.11	0.27	0.56	0.43	0.81	0.47	0.44	0.29	0.42	0.59
K_2O	8.79	8.53	8.16	8.00	6.5	7.52	7.97	8.18	9.61	9.59	9.78
Total	94.76	94.75	94.27	94.45	94.96	94.38	94.19	94.47	100.00	100.00	100.00
					11O						
Si	2.76	2.77	2.75	2.81	2.73	2.70	2.71	2.72	2.72	2.73	2.73
Ti	0.07	0.07	0.06	0.07	0.07	0.09	0.09	0.09	0.02	0.03	0.04
Al(VI)	1.24	1.23	1.25	17.19	1.27	1.30	1.29	1.29	1.28	1.27	1.27
Al(IV)	0.30	0.26	0.26	0.37	0.26	0.39	0.39	0.43	0.53	0.53	0.50
Cr	–	0.02	0.07	0.01	0.03	0.01	0.01	0.02	–	–	–
Fe^{2+}	1.72	1.81	1.80	0.85	0.98	1.09	1.09	1.12	0.93	0.89	0.90
Mn	0.01	0.01	0.01	–	–	–	–	–	0.01	–	0.02
Mg	0.81	0.77	0.74	1.60	1.60	1.27	1.27	1.22	1.41	1.42	1.40
Ca	–	0.01	0.03	0.01	0.01	–	–	–	–	–	–
Na	0.02	0.02	0.04	0.08	0.06	0.68	0.68	0.07	0.04	0.06	0.08
K	0.89	0.87	0.84	0.76	0.61	0.77	0.77	0.79	0.87	0.86	0.88
Zn	–	0.01	–	0.01	–	–	–	0.01	–	–	–
Cl	–	–	–	0.01	–	–	–	0.02	0.01	–	0.01
X_{Fe}	0.68	0.70	0.71	0.35	0.38	0.47	0.47	0.48	0.40	0.39	0.39

Table 7. (Contd.)

Component	5264/212				5262/100		5257/23.2				
	Bt-20	*Bt*-33	*Bt*-37	*Chl*-21	*Chl*-57	*Bt*-58	*Bt*-38	*Bt*-39	*Bt*-40	*Bt*-43	*Bt*-44
	core	margin	matrix		core	margin	margin	core	margin	core	margin
		Crd				*Cru*	*Crt*	inclusion in *Grt*			
SiO_2	35.27	43.75	35.03	37.39	25.33	30.34	36.96	39.04	37.89	38.42	37.21
TiO_2	1.18	1.14	1.29	0.45	0.24	0.63	1.23	1.21	1.19	1.24	1.05
Al_2O_3	19.95	17.82	19.23	34.61	18.82	15.19	17.97	18.62	18.18	18.42	18.73
Cr_2O_3	0.16	0.42	0.08	0.11	0.19	1.98	0.27	0.24	0.45	0.21	0.31
FeO	20.36	17.24	19.92	6.27	39.83	35.46	15.01	14.53	14.32	15.03	14.43
MnO	–	0.02	–	0.01	0.04	0.12	0.02	–	0.05	0.12	–
MgO	10.72	9.12	10.57	6.86	5.43	4.49	15.36	15.89	15.07	15.15	15.24
CaO	0.08	0.05	0.01	0.26	0.06	0.17	0.14	0.04	0.11	0.03	–
ZnO	0.13	0.37	–	–	–	–	0.09	0.05	0.02	–	0.05
ClO	0.05	0.09	0.09	0.02	0.14	0.29	0.16	0.11	0.08	0.04	0.07
Na_2O	0.46	0.45	0.42	1.91	0.19	0.21	0.75	0.48	0.45	0.43	0.05
K_2O	8.26	7.12	8.33	0.03	1.44	5.50	7.69	7.73	7.71	7.96	8.14
Total	96.62	97.59	95.03	88.96	91.72	94.37	95.60	97.94	95.54	97.10	95.76
	11O			14O			11O				
Si	2.64	3.11	2.66	3.39	2.79	2.44	2.70	2.77	2.76	2.76	2.72
Ti	0.07	0.06	0.07	0.03	0.02	0.04	0.07	0.06	0.07	0.07	0.06
Al(IV)	1.36	0.89	1.34	0.61	1.21	1.44	1.30	1.24	1.24	1.24	1.28
Al(VI)	0.39	0.61	0.39	3.09	1.23	–	0.25	0.32	0.33	0.32	0.33
Cr	0.01	0.02	0.01	0.01	0.02	0.13	0.02	0.01	0.03	0.01	0.02
Fe^{3+}	–	–	–	–	0.45	–	–	–	–	–	–
Fe^{2+}	1.19	1.03	1.19	1.07	6.82	1.44	0.75	0.72	0.79	0.79	0.78
Mn	–	–	–	–	–	0.01	–	–	–	0.01	–
Mg	1.19	0.97	1.20	0.93	0.89	0.54	1.68	1.68	1.64	1.62	1.66
Ca	0.01	–	–	0.02	0.01	0.01	0.01	–	0.01	–	–
Zn	0.01	0.02	–	–	–	–	0.01	–	–	–	–
Cl	–	0.01	–	–	0.02	–	–	–	–	–	–
Na	0.07	0.06	0.07	0.34	0.04	0.03	0.11	0.07	0.06	0.06	0.08
K	0.79	0.65	0.81	–	0.20	0.56	0.72	0.70	0.72	0.73	0.76
X_{Fe}	0.52	0.52	0.51	0.34	0.81	0.82	0.35	0.34	0.35	0.36	0.35

Table 8. Composition (wt %) of feldspars from metapelites of the Prioskol'skaya area

Component	5264/212				5262/100			5264/228			5257/20	5420/6		
	Pl-22	*Pl*-29	*Pl*-30	*Pl*-31	*Pl*-52	*Pl*-53	*Pl*-56	*Pl*-3	*Pl*-5	*Pl*-6	*Kfs*-27	*Pl*-48	*Pl*-51	*Pl*-52
	core	margin	core	margin	core	margin	core	margin	core	margin				
SiO_2	66.50	67.96	67.34	67.51	62.75	64.18	65.09	68.78	68.72	68.00	46.52	61.04	61.74	61.35
Al_2O_3	21.64	21.63	21.31	21.85	21.76	23.16	22.76	20.07	20.93	20.64	38.79	24.40	24.24	23.76
FeO	0.09	0.03	0.03	0.12	4.17	0.08	0.09	0.13	0.05	0.13	0.42	0.19	0.12	0.03
CaO	1.49	0.77	1.27	1.28	2.56	2.92	2.76	0.68	0.32	0.36	0.40	6.16	5.70	5.22
ClO	0.01	–	0.07	0.01	0.05	0.02	0.03	0.05	0.04	0.02	0.04	0.02	–	–
Na_2O	10.19	10.18	10.02	9.93	8.54	9.43	9.41	10.07	10.41	10.32	0.18	8.09	8.11	7.46
K_2O	0.02	0.01	0.02	0.06	0.06	0.03	0.06	0.04	0.02	0.03	10.41	0.04	0.08	2.03
Total	99.93	100.59	99.99	100.8	99.90	99.84	100.21	99.90	100.49	99.81	97.19	99.99	99.99	99.99
8O														
Si	2.91	2.94	2.94	2.92	2.81	2.85	2.85	2.99	2.98	2.98	2.19	2.71	2.737	2.741
Al	1.12	1.10	1.09	1.12	1.13	1.18	1.17	1.04	1.07	1.05	2.15	1.28	1.27	1.25
Fe	–	–	–	0.04	0.15	–	–	0.01	–	0.01	0.02	0.01	–	–
Ca	0.07	0.04	0.06	0.06	0.12	0.14	0.13	0.03	–	0.02	0.02	0.29	0.27	0.250
Cl	–	–	0.01	–	–	–	–	–	–	–	–	–	–	
Na	0.86	0.85	0.85	0.83	0.73	0.79	0.80	0.85	0.88	0.87	0.02	0.70	0.70	0.65
K	–	–	–	–	–	–	–	–	–	–	0.63	–	0.01	0.12
Ab	0.92	0.96	0.93	0.93	0.86	0.85	0.86	0.96	1.00	0.98	0.03	0.70	0.72	0.64
An	0.08	0.04	0.07	0.7	0.14	0.15	0.14	0.04	–	0.02	0.03	0.30	0.28	0.25
Ort	–	–	–	–	–	–	–	–	–	–	0.98	–	0.01	0.11

Table 9. Composition (wt %) of spinel, magnetite, and talc from metapelites of the Prioskol'skaya area

Component	5257/20		5267/290					
	Spl-1	*Spl*-2	*Spl*-7	*Spl*-10	*Spl*-52	*Mag*-54	*Tlc*-4	*Tlc*-11
	in aggregates with *And* and *Sil*		in aggregates with *Mag*				replaces *Ol*	
SiO_2	–	–	0.01	–	0.02	0.03	44.10	49.30
TiO_2	–	–	0.01	–	0.02	0.20	0.03	–
Al_2O_3	57.34	58.40	59.03	59.35	60.43	0.55	0.04	0.02
Cr_2O_3	0.02	0.02	–	–	0.05	0.04	0.14	0.04
FeO	31.80	28.90	32.67	32.32	31.16	99.00	27.24	12.19
MnO	0.22	0.33	0.01	0.11	0.09	0.08	0.14	0.07
MgO	6.57	7.66	8.24	8.19	8.13	0.05	17.41	30.24
CaO	–	–	–	0.01	0.03	0.01	0.20	0.05
ClO	–	–	–	–	0.02	0.01	0.03	–
ZnO	3.96	3.67	–	–	–	–	–	–
V_2O_5	0.15	0.16	–	–	–	–	–	–
Total	100.01	99.14	100.00	100.02	99.96	100.00	89.34	91.93
			4 O				10 O	
Si	–	–	–	–	–	–	3.53	3.52
Ti	–	–	–	–	–	0.01	–	–
Al	1.94	1.92	1.91	1.92	1.95	0.02	–	–
Cr	–	–	–	–	–	–	0.01	–
Fe^{3+}	0.10	0.07	0.66	0.66	0.05	1.00	–	–
Fe^{2+}	0.65	0.60	0.09	0.08	0.66	1.96	1.82	0.73
Mn	0.01	0.01	–	–	–	–	0.01	–
Mg	0.27	0.32	0.34	0.34	0.33	–	2.08	3.22
Ca	–	–	–	–	–	–	0.02	–
Cl	–	–	–	–	–	–	–	–
Zn	0.08	0.08	–	–	–	–	–	–
V	–	–	–	–	–	–	–	–
X_{Fe}	0.80	0.79	0.69	0.69	0.92	1.00	0.47	0.18

in diameter. Its X_{Fe} varies from 84.6 to 86.0 (Table 6). The MnO and CaO concentrations are insignificant, no higher than 0.5 wt %. No clear-cut chemical zoning was detected.

Garnet in the metapelites of the muscovite–sillimanite zone (Sample 5257/20) composes large (up to 0.8 mm) porphyroblasts. Numerous graphite and biotite inclusions in the garnet of this sample compose so-called S-shaped textures. In contact with large garnet crystals, smaller grains occur (no larger than 0.2 mm), which are analogous to those in the rock groundmass. They contain no inclusions, their faces cut across the schistosity, and these grains have no pressure shadows nearby. The large garnet has X_{Fe} = 78.3% in the core and 75.5% in the margin. No pronounced chemical zoning was detected in small grains (Fig. 5c), whose X_{Fe} is close to that in the peripheral portions of the large garnet crystal, 76.4–76.2% in the core and 77.0–76.5% in the margin.

Biotite is the dominant Fe–Mg silicate of all metapelites in the Prioskol'skaya structure. Its amounts vary from 5–10 to 40%, and its sizes are from 0.2–0.5 to 3–4 mm. Biotite sometimes occurs as inclusions in garnet. The biotite of the staurolite–sillimanite zone has X_{Fe} = 46.1–51.6% (Table 7). A somewhat more magnesian composition was detected in the biotite from the muscovite–sillimanite zone (Samples 5257/20 and 5420/6), X_{Fe} = 34.7–39.8%, perhaps, because of the differences between the bulk-rock compositions. The biotite from the staurolite–sillimanite zone contains 1.11–1.64 wt % TiO_2, and this mineral from the muscovite–sillimanite zone has 1.02–1.83 wt % TiO_2.

Spinel develops as small (no more than 1 mm) green crystals, which occur in the metapelites (Sample 5257/20)

Table 10. Representative analyses (wt %) of staurolite from metapelites of the Prioskol'skaya area

Component	5264/228				5264/212				
	St-1	*St*-7	*St*-8	*St*-4	*St*-23	*St*-24	*St*-27	*St*-34	*St*-36
	core	margin	margin	margin	core	margin	core	core	core
			Grt	*Sil*	small grains in a *Crd* rim				
SiO_2	27.88	26.32	27.12	26.70	26.06	26.52	26.39	26.46	26.32
TiO_2	0.36	0.45	0.48	0.45	0.15	0.14	0.07	0.23	0.13
Al_2O_3	55.46	56.98	56.77	55.99	55.13	53.49	54.96	53.58	55.39
Cr_2O_3	0.09	0.15	0.17	–	0.04	0.14	0.09	0.21	0.08
FeO	14.57	14.54	14.93	14.82	15.93	15.64	15.81	16.25	15.83
MnO	0.01	–	0.01	0.03	0.06	0.17	0.03	0.12	0.05
MgO	1.62	1.48	1.51	1.56	1.59	1.37	1.67	1.73	1.50
CaO	–	0.01	–	0.01	–	0.03	–	0.04	0.02
ClO	–	–	–	–	0.02	0.04	0.02	0.04	0.03
ZnO	0.14	–	0.08	–	0.08	0.29	0.38	0.35	0.14
Na_2O	–	0.03	–	–	0.05	0.12	0.02	0.03	0.04
K_2O	–	–	0.01	–	0.01	0.04	–	0.02	0.03
Total	99.13	99.94	99.97	99.56	99.11	97.99	99.45	99.08	99.58
				46 O					
Si	7.58	7.37	7.1	7.13	7.35	7.46	7.49	7.57	7.46
Ti	0.07	0.09	0.10	0.09	0.03	0.03	0.02	0.05	0.03
Al	17.77	18.11	18.29	18.09	17.96	17.72	17.72	17.40	17.81
Cr	0.02	0.03	0.04	–	0.01	0.03	0.02	0.05	0.02
Fe	3.31	3.28	3.41	3.40	3.62	3.68	3.62	3.47	3.61
Mn	–	–	–	0.01	0.01	0.04	0.01	0.03	0.01
Mg	0.66	0.59	0.62	0.64	0.64	0.58	0.68	0.71	0.61
Ca	–	–	–	0.03	–	0.01	–	0.01	0.01
Zn	0.03	–	0.01	–	0.02	0.06	0.08	0.07	0.03
Cl	–	–	–	–	0.01	0.02	0.01	0.02	0.01
Na	–	0.16	–	–	0.03	0.06	0.01	0.02	0.02
K	–	–	–	–	0.01	0.01	–	0.01	0.01
X_{Fe}	0.83	0.85	0.85	0.84	0.85	0.86	0.84	0.83	0.86

in association with garnet and andalusite and is a decomposition product of staurolite in the absence of quartz. Spinel inclusions are contained in large andalusite crystals (Fig. 3f), in which it corresponds to hercynite with a high ZnO concentration, 3.67–3.96 wt % (Table 9).

Plagioclase is present in most of the samples as small untwined crystals. The plagioclase of the staurolite-bearing schists is albite with a minute anorthite admixture. In Sample 5264/228, this is nearly pure unzoned albite ($Ab_{96.5–97.7}An_{2.3–3.5}$; Table 8). The plagioclase of Sample 5420/6 occurs as larger twinned crystals of oligoclase–andesine composition ($Ab_{63.9–71.7}An_{24.7–29.5}$).

Potassium feldspar occurs in the metapelites of the Prioskol'skaya area in the high-temperature part of the muscovite–sillimanite zone. This mineral is present in Sample 5257/20 in assemblage with garnet, biotite, and spinel is orthoclase with minor albite and anorthite concentrations ($Ort_{94.5}An_{3.1}Ab_{2.5}$; Table 8).

Andalusite is contained in the metapelites more rarely than sillimanite within the staurolite–sillimanite and the low-temperature part of the muscovite–sillimanite zone. In the quartz-free rocks, andalusite composes large (up to 4 mm) crystals (Fig. 3f) in association with garnet and spinel. Some zones of andalusite crystals are often replaced by sillimanite-fibrolite. Andalusite sometimes composes large porphyroblasts with numerous inclusions of quartz and biotite with the development of skeletal shapes (Sample 5420/6). Large

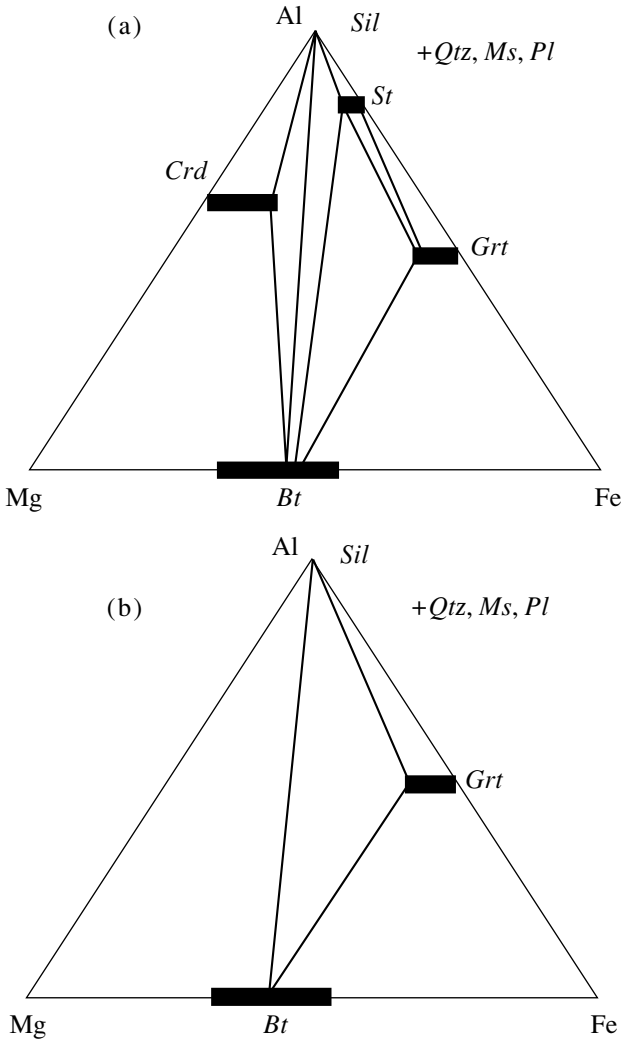

Fig. 6. Mineral equilibria in K_2O-rich metapelites of the Prioskol'skaya area.
(a) Staurolite–sillimanite zone; (b) sillimanite–muscovite zone.

andalusite porphyroblasts are often replaced in the margins by sillimanite prisms.

Sillimanite is spread quite widely in the rocks and replaces andalusite or muscovite. Andalusite rhombs are often replaced by sillimanite (Fig. 3f). In association with staurolite, sillimanite occurs as small prismatic crystals (no larger than 0.5 mm) and smaller amounts of fibrolite.

Muscovite is present in the rocks fairly often, usually in the form of flakes, platelets, and laths, whose sizes increase from the staurolite–sillimanite to the muscovite–sillimanite zone. Secondary fine-flaky muscovite is diaphthoretic phase, replacing mostly feldspars.

INTERPRETATION OF MINERAL EQUILIBRIA

The K_2O-rich metapelites of the area contain textural evidence of a series of prograde reactions, which

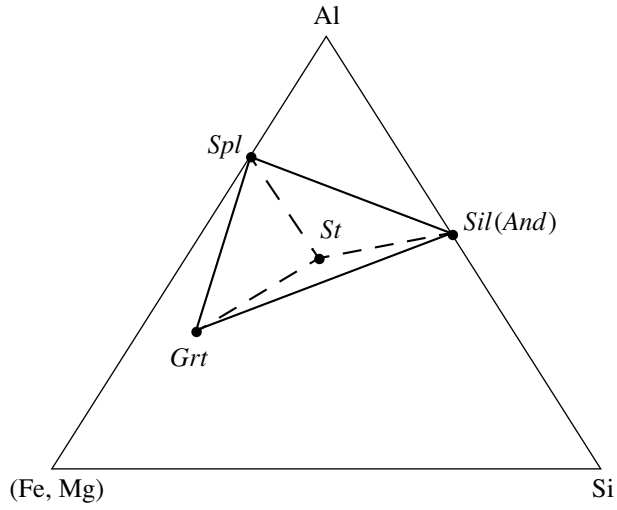

Fig. 7. Staurolite decomposition into spinel, sillimanite, and garnet.

make it possible to distinguish the following three subfacies: staurolite–sillimanite, muscovite–sillimanite, and muscovite–sillimanite–potassic feldspar.

Staurolite–Sillimanite Zone

The low-temperature boundary of the staurolite–sillimanite zone is the first appearance of sillimanite and the simultaneous breakdown of the last chlorite, which may remain stable in assemblage with manganous garnet up to the staurolite–sillimanite zone,

$$St + Ms + Chl \longrightarrow Bt + Sil + Qtz + H_2O. \quad (1)$$

This reaction results in the origin of the biotite–sillimanite assemblage (Fig. 6a). As soon as the last chlorite disappears (it decomposes in rocks rich in iron long before the appearance of sillimanite), the stability field of staurolite within the staurolite zone starts progressively diminishing, and the X_{Mg} of the garnet increases due to the reactions

$$St + Ms + Qtz \longrightarrow Bt + Sil + Grt + H_2O \quad (2)$$

and

$$Grt_{Fe} + Ms \longrightarrow Grt_{Mg-Fe} + Bt + Sil, \quad (3)$$

so that the *Bt* + *Sil* + *Grt* assemblage shifts to the left in the diagram of Fig. 6a with increasing temperature.

Very important reaction textures of the metapelites are those of the prograde staurolite decomposition into andalusite, sillimanite, and spinel in quartz-free rocks (Sample 5257/20; Fig. 7) near the high-temperature boundary of the staurolite–sillimanite facies in accordance with the reaction

$$St \longrightarrow Sil\ (And) + Spl + Grt + H_2O. \quad (4)$$

In K_2O-poor, relatively Fe-rich metapelites, this reaction is associated with the development of monomineralic cordierite rims around staurolite, which are

widespread in Sample 5264/212 (Fig. 3e). Their development reflects the prograde reaction

$$St_{Mg-Fe} + Qtz \longrightarrow St_{Fe} + Crd + Sil + H_2O. \quad (5)$$

The disappearance of staurolite by the reaction *St* + *Ms* + *Qtz* ⟶ *Bt* + *Sil* + *Grt* + H_2O is accompanied by andalusite replacement by fibrolite (Fig. 6a). The metapelites of the Prioskol'skii zonal complex contain sillimanite of two types: (1) replacing andalusite by means of the normal polymorphic transformation and (2) replacing muscovite by the reaction

$$St + Chl + Ms \longrightarrow Bt + Sil + Qtz + H_2O,$$

which explains the development of characteristic interlaced aggregates of biotite and sillimanite.

The K_2O-poor, moderately aluminous rocks with the $Ged_{49} + Ath_{41} + Crd_{34} + Bt_{51} \pm Sil \pm Grt_{65} \pm Qtz$ contain no staurolite because of the magnesian bulk-rock chemistry, while the staurolite of the complex is high in Fe (X_{Fe} > 83%, Table 10). The rocks never simultaneously contain gedrite and anthophyllite together with cummingtonite. It can be proposed that the *Ged* + *Ath* + *Crd* assemblage is produced during the prograde decomposition of medium-Fe chlorite

$$Chl \longrightarrow Ath + Ged + Crd + Sil + H_2O. \quad (6)$$

Muscovite–Sillimanite Zone

The muscovite–sillimanite zone in the K_2O-rich metapelites can be distinguished by the complete disappearance of staurolite and the broad stability of the *Qtz* + *Bt* + *Ms* + *Sil* ± *Grt* assemblage (Fig. 6b).

In K_2O-poor rocks, a temperature increase is associated with the replacement of the early assemblage of *Ged* + *Sil* by the higher temperature assemblage *Grt* + *Crd* (Fig. 8) by the reaction

$$Ged + Sil + Qtz \longrightarrow Grt + Crd + H_2O. \quad (7)$$

This reaction proceeds in the Prioskol'skii Complex within the muscovite–sillimanite zone, closer to the potassium feldspar isograde. Our rocks bear both stable assemblages, but the *Grt-Crd* association is more common, which suggests that the equilibrium was shifted to the right-hand side (Fig. 8). Conceivably, the coexistence of certain assemblages within a rock is facilitated by additional components, such as Na in gedrite and Ca and Mn in garnet.

The sillimanite-free gedrite–anthophyllite–cordierite–garnet rocks contain newly formed orthopyroxene. The relations between the X_{Fe} of the minerals of this rock are as follows: $Crd_{22-34} < Opx_{39.5} < Ath_{40-43} < Ged_{46-49} < Grt_{65-79}$. The close X_{Fe} values of the anthophyllite and orthopyroxene suggest that the latter mineral was produced by the partial prograde decomposition of anthophyllite

$$Ath \longrightarrow Opx + Qtz + H_2O. \quad (8)$$

According to our observations, orthopyroxene appears in the muscovite–sillimanite zone, in which the rare *Ol–Ged–Opx–Grt–Mag* assemblage was also encountered.

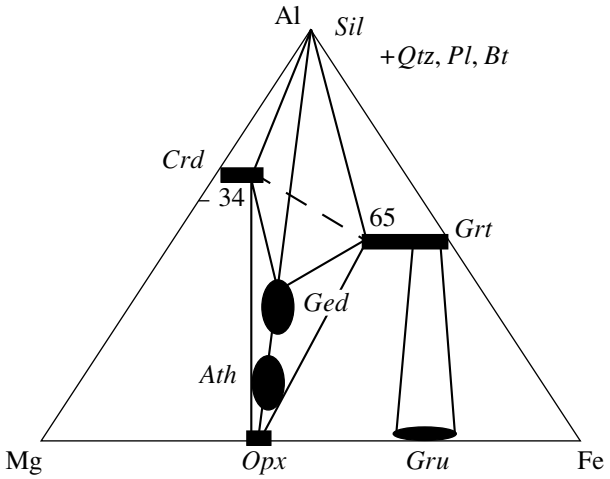

Fig. 8. Mineral equilibria in K_2O-poor metapelites of the Prioskol'skaya area.

A further temperature increase leads to the appearance of potassic feldspar in K_2O-rich metapelites due to the partial decomposition of muscovite

$$Ms_{K-Na} + Qtz \longrightarrow Ms_K + Kfs + Sil, \quad (9)$$

with muscovite simultaneously fully disappearing from the mineral assemblages.

OLIVINE–GEDRITE–ORTHOPYROXENE–GARNET–MAGNETITE ASSEMBLAGE

Olivine is a very rare mineral in K_2O- and CaO-poor rocks. Forsterite was occasionally found with sapphirine in high-Al magnesian rocks (Grew *et al.*, 1994) and with cordierite in metamorphosed peridotites in contact aureoles (Arai, 1975). The fayalite plus cordierite assemblage was documented in Fe-rich hornfels (Abraham and Schreyer, 1973; Sawaki, 1990; Anan'ev and Reverdatto, 1997). The *P–T* stability parameters were calculated by Seifert (1974), Herzberg (1983), and Anan'ev *et al.* (1997) for olivine with cordierite and by Grew *et al.* (1994) for cordierite with sapphirine.

The *Ol–Ged–Opx–Grt–Mag* assemblage was found in quartz-free K_2O-poor magnesian metapelites (Sample 5267/290), which were metamorphosed to the amphibolite facies in the muscovite–sillimanite zone. We are aware of only one description of the olivine plus gedrite assemblage: in metamorphosed olivine dolerite (Otten, 1984), in which gedrite occurs in interlaced aggregates with hornblende in the second layer of the reaction corona (its first layer consists of orthopyroxene and magnetite), between plagioclase and olivine. The olivine is fully replaced by a cummingtonite–magnetite aggregate.

The *P–T* parameters of the stability field of olivine with gedrite cannot be accurately calculated because of

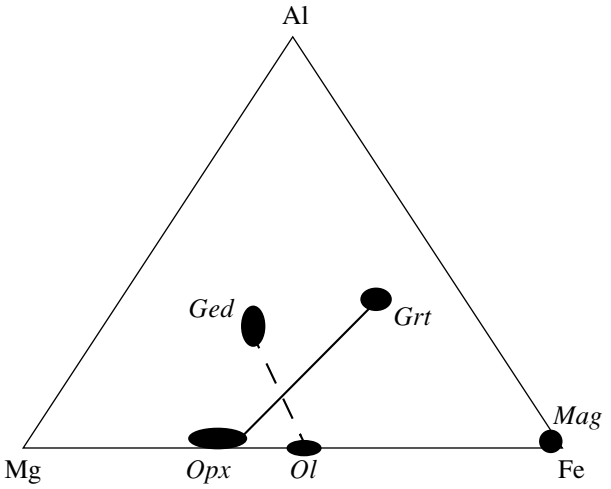

Fig. 9. Mineral equilibria in olivine-bearing metapelite of the Prioskol'skaya area. Solid tie-line illustrates the reaction $Ol + Ged \longrightarrow Opx + Grt + H_2O$.

the uncertainty in the thermodynamic properties of gedrite, particularly considering the facts that natural gedrites commonly contain Na_2O (in amounts up to 1 f.u.) and the instability of the end members, Mg- and Fe-gedrite (Fischer *et al.*, 1999).

Sample 5267/290 contains an unusual quartz-free assemblage of ferrous olivine (X_{Fe} = 51–56%) with pyrope–almandine garnet, gedrite, orthopyroxene, and magnetite (with inclusions of Fe-hercynite). The assemblage seems to be generally equilibrated (Figs. 3a, 3b), although the garnet is more euhedral than the olivine and, perhaps, it grew simultaneously with the partial resorption of the olivine. The proposed reaction (Fig. 9) is largely consistent with prograde reactions in the K_2O-rich metapelites

$$Ged + Ol \longrightarrow Opx + Grt + H_2O. \quad (10)$$

Vermicular magnetite inclusions in the garnet, gedrite, and orthopyroxene (Fig. 3b) seem to indicate that the magnetite amounts in the rock increased in the course of the prograde metamorphism because of an increase in the oxygen fugacity and the decomposition of some silicates (with an increase in their X_{Mg}) by the reaction

$$\text{Fe–Mg silicate} + O_2 \longrightarrow \text{Mg–Fe silicate} + Mag \pm Spl. \quad (11)$$

PHASE EQUILIBRIA OF COEXISTING ORTHOAMPHIBOLES

Anthophyllite and gedrite coexist in our cordierite–orthoamphibole schists as two individual phases. The existence of a miscibility gap of orthoamphiboles between low-Al anthophyllite and high-Al gedrite was discussed by several researchers (Robinson *et al.*, 1969; Robinson and Jaffe, 1971; Spear, 1980; Stoddard and Miller, 1990; and others). It is generally thought that the gap exists at temperatures below 630°C and disappears at higher temperatures, but, in spite of this conclusion, the equilibrium coexistence of anthophyllite and gedrite remains uncertain.

Isomorphism in the orthoamphiboles can be described by the following three mechanisms: Fe $\rightleftharpoons$ Mg (Fe–Mg exchange), Al(VI)Al(IV) $\rightleftharpoons$ MgSi (Tschermak's replacement), and NaAl(IV) $\rightleftharpoons$ Si (edenitic replacement). Other replacement mechanisms, including such elements as Mn, Ti, Fe^{3+}, or Ca are less important and are not considered here.

The main difference of gedrite from anthophyllite lies in the intensity of the second- and third-type replacements: the miscibility gap between the minerals is caused by the different distribution of these isomorphic components.

The anthophyllite–gedrite immiscibility in the Prioskol'skaya rocks is clearly illustrated in Fig. 10 and is expressed in the different concentrations of alumina and alkalis in these minerals. The Al(VI) concentration is 0.60–0.10 f.u. in the anthophyllite and 1.4 ± 0.2 in the gedrite; and their Al(IV) contents are, respectively, 0.12–0.59 and 0.97–1.42 f.u.

Figure 10 demonstrates correlations between Al(VI) with Mg (Fig. 10a) and Fe (Fig. 10b) in the coexisting anthophyllite and gedrite. The anthophyllite is characterized by somewhat elevated concentrations of MgO compared with those in the gedrite. The miscibility gap in terms of X_{Fe} of the coexisting orthorhombic amphiboles is narrow, with this parameter equal to 44 at. % for the anthophyllite and 46 at. % for the gedrite. The gedrite in association with olivine (Sample 5267/290) has a relatively low X_{Fe}, 40 at. %.

Figure 10c demonstrates the correlation between the concentrations of alkalis and X_{Fe} [X_{Fe} = Fe/(Fe + Mg), at. %] in the subalkaline anthophyllite and gedrite: the anthophyllite is low in K and Na (contains no more than 0.15 f.u.), whereas the gedrite contains them in amounts of 0.30–0.45 f.u.

Fe-richer lithologies contain grunerite (in place of both anthophyllite and gedrite) in association with almandine (X_{Fe} = 0.93 at. %). The gedrite and anthophyllite coexisting with relatively magnesian garnet (X_{Fe} = 0.79 at. %) have 550°C = 0.46–0.47 and 0.40–0.43 at. %, respectively. More magnesian orthoamphiboles can coexist with cordierite (Samples 5267/290, 5257/23.1, and 5257/22). The most aluminous anthophyllite are in association with gedrite, and the most aluminous gedrite coexists with cordierite.

The higher temperature rocks usually contain orthopyroxene in association with gedrite, while the lower temperature varieties bear cordierite commonly with anthophyllite.

Based on garnet–biotite and garnet–orthopyroxene temperature estimates for the magnesian metapelites with coexisting orthoamphiboles (Tables 11, 13), it can be concluded that the miscibility gap between antho-

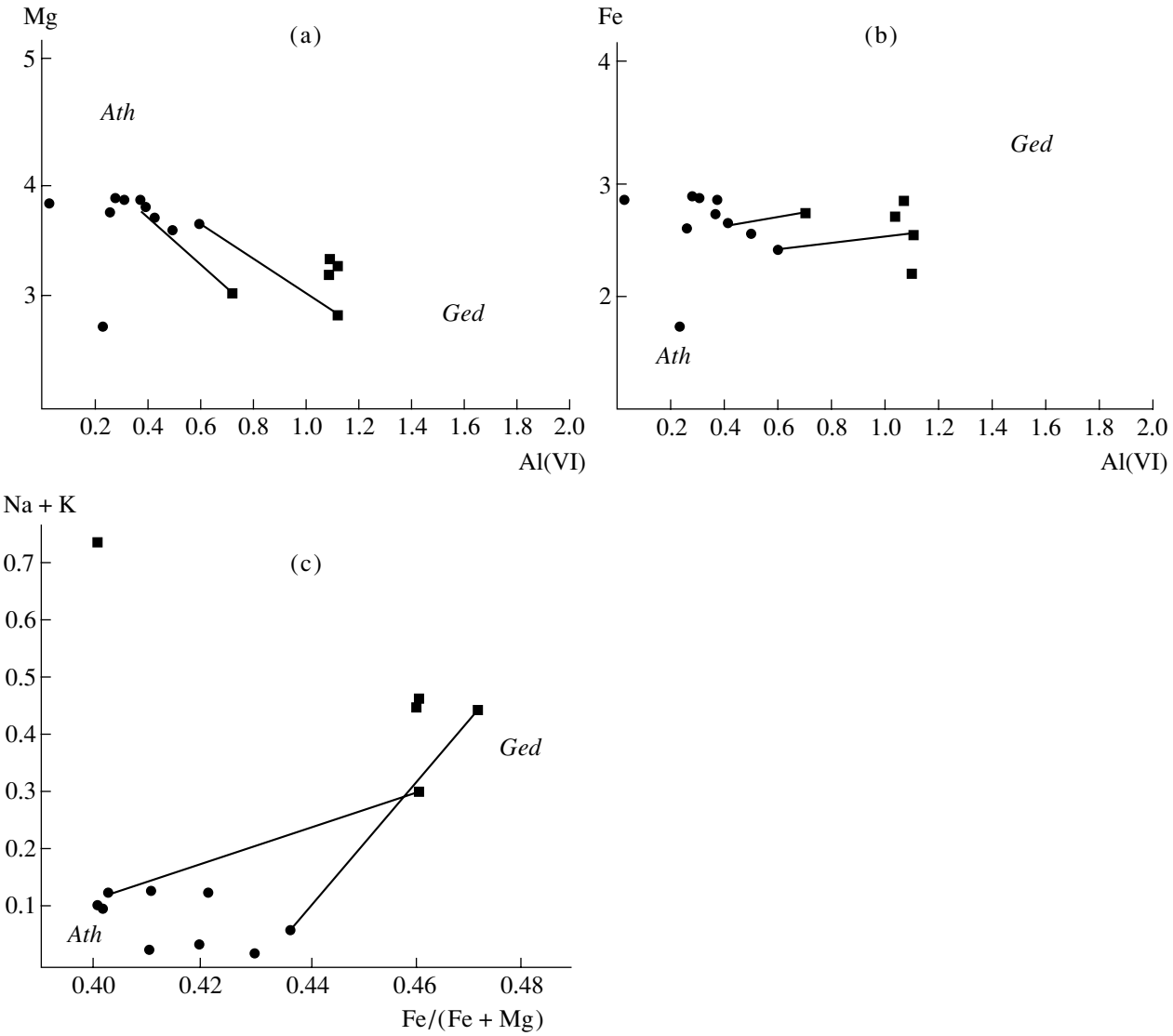

Fig. 10. Correlations between major components (f.u.) in coexisting anthophyllite and gedrite of the Prioskol'skaya area. (a) Correlation between Mg and Al(VI); (b) correlation between Fe and Al(VI); (c) correlation between (Na + K) and X_{Fe}.

phyllite and gedrite is between 550 and 630°C, which is consistent with the conclusions made by Spear (1980) and Robinson *et al.* (1982).

METAMORPHIC *P–T* CONDITIONS

The *P–T* parameters of metamorphism of the Prioskol'skaya metapelites were refined using two groups of techniques. One of them involved the comparison of the mineral assemblages of these rocks with known petrogenetic grids (Korikovsky, 1979; Powell and Holland, 1990; Spear and Cheney, 1989; Xu *et al.*, 1994; and others) and experimental data on the stability of various minerals and mineral assemblages (for example, aluminum silicates, staurolite with quartz, muscovite with quartz, etc.). These techniques make it possible to determine the general position of the assemblages in question in *P–T* diagrams and to identify the type of the metamorphic facies series. It can be particularly successfully applied to medium-temperature metapelites, in which a relatively narrow temperature interval comprises a succession of appearing and decomposing minerals (such as chlorite, staurolite, and muscovite) with systematic variations in their composition.

The utilization of mineralogical thermobarometry based on microprobe analyses of minerals and their chemical zoning enables one to more precisely pinpoint the *P–T* parameters of individual samples, particularly when they contain zoned mineral grains, and reproduce the *P–T* trajectories of the rocks.

The presence of the staurolite plus sillimanite assemblage in the metapelites definitely points to intermediate pressures (3–5 kbar). Because the metapelites

Table 11. Estimated metamorphic temperatures of metapelites from the Prioskol'skaya area, biotite–garnet thermometer, pressure equals 4 kbar

Sample	*Grt-Bt* pair	*Grt-Bt* thermometer				T_{aver}, °C
		T	*HL*	*LP*	*P*	
Staurolite–sillimanite zone						
5264/228	*Grt*(1)-*Bt*(2)	553	544	568	551	554 ± 14
	Grt(2)-*Bt*(4)	529	518	544	533	531 ± 13
Muscovite–sillimanite zone						
5257/20	*Grt*(18)-*Bt*(26)	542	534	550	538	541 ± 19
	Grt(19)-*Bt*(25)	564	554	563	550	558 ± 8
	Grt(20)-*Bt*(25)	568	557	573	558	564 ± 13
	Grt(21)-*Bt*(26)	561	551	560	547	555 ± 8
	Grt(22)-*Bt*(25)	571	560	573	559	567 ± 8
	Grt(23)-*Bt*(26)	567	557	572	558	563 ± 6
5422/16	*Grt*(9)-*Bt*(19)	547	539	533	541	540 ± 7
	Grt(15)-*Bt*(20)	578	566	576	561	570 ± 9
	Grt(17)-*Bt*(23)	570	559	574	560	567 ± 8
5257/23.2	*Grt*(14)-*Bt*(39)	616	599	611	593	605 ± 12
	Grt(12)-*Bt*(38)	565	554	569	555	561 ± 8
	Grt(22)-*Bt*(44)	617	600	614	596	607 ± 11
	Grt(13)-*Bt*(40)	627	609	620	601	614 ± 11
	Grt(30)-*Bt*(43)	646	626	637	617	632 ± 15

Note: Geothermometers: *T* (Thompson, 1976), *HL* (Holdaway and Lee, 1977), *LP* (Lavrent'eva and Perchuk, 1981), *P* (Perchuk *et al*., 1984).

Table 12. Estimated metamorphic temperatures and pressures of metapelites from the Prioskol'skaya area, *Grt–Pl*–Al_2SiO_5–*Qtz* and *Grt–Opx* thermobarometry

Sample	Assemblage and analysis nos. in Tables 1, 3, 5, 8	T_{aver}, °C	Barometers			
			GASP		*Grt-Opx*	
			AP(1)	*AP*(2)	*AK*	*H*
Staurolite–sillimanite zone						
5264/228	*Grt*(1)-*Pl*(5)-*Qtz*-(*Sil*)	550	6.2	5.2	–	–
	Grt(2)-*Pl*(6)-*Qtz*-(*Sil*)	550	4.3	3.3		
Muscovite–sillimanite zone						
5257/23.2	*Grt*(12)-*Opx*	600			4.5	3.3
	Grt(38)-*Opx*	600			5.1	4.1

		Thermobarometers *Grt-Opx*			
		AK		*AP*(2)	
		T	*P*	*T*	*P*
5257/23.2	*Grt*(12)-*Opx*(47)	554	5.0	548	4.0

Note: Thermometers and barometers: *Grt-Pl*-Al_2SiO_5-*Qtz* (*GASP*) and *Grt–Opx* barometers: *AP*(1) (Aranovich and Podlesskii, 1980), *AK* (Aranovich and Kosyakova, 1987), *AP*(2) (Aranovich and Podlesskii, 1989), *H* (Harley, 1984).

of the staurolite–sillimanite zone were penetrated by only one hole, we failed to constrain the low-temperature *P–T* boundary of this zone. Garnet–biotite thermometry on the rocks yielded 531–554°C (Table 11). The pressure was evaluated for Sample 5264/228, which contained the assemblage *Bt* + *Qtz* + *Grt* + *Pl* + *St* + *Sil* and, hence, offered the possibility of using the garnet–plagioclase–quartz–sillimanite geobarometer

Table 13. Estimated metamorphic temperatures of metapelites from the Prioskol'skaya area, garnet–cordierite and garnet–orthopyroxene thermometers, pressure equals 4 kbar

Sample	Assemblage and analysis nos. in Tables 1, 2, 4–8	Thermometer							
		Grt-Opx				*Grt-Crd*			
		AK	*LP*	*B*	*LG*	*T*	*HL*	*LP*	*P*
5257/23.2	*Grt*(12)-*Opx*(47)	552	509	553	561	–	–	–	
	Grt(38)-*Opx*(47)	613	573	563	578	–	–	–	
5257/22	*Grt*(1)-*Crd*(7)					714	684	676	723
	Grt(2)-*Crd*(8)					687	666	656	701
	Grt(5)-*Crd*(9)	–	–			659	642	635	653
	Grt(8)-*Crd*(10)	–	–			683	663	655	699
5267/290	*Grt*(50)-*Opx*(14)	641	606	641	670				
	Grt(32)-*Opx*(51)	593	568	591	597				
	Grt(2)-*Opx*(3)	610	588	607	621				
	Grt(11)-*Opx*(2)	528	550	549	550				

Note: Thermometers: *P* (Perchuk, 1989), *AK* (Aranovich and Kosyakova, 1987), *T* (Thompson, 1976), *HL* (Holdaway and Lee, 1977), *LP* (Lavrent'eva and Perchuk, 1981), *P* (Perchuk *et al.*, 1984), *B* (Bhattacharya *et al*., 1991), *LG* (Lee and Ganguly, 1988).

(Aranovich and Podlesskii, 1980). The retrieved values lie within the range of 4–6 kbar (Table 12) and are in good agreement with the results of the chemographic paragenetic analysis. Sample 5257/20 was determined to contain the assemblage of spinel with andalusite, sillimanite, and garnet, which was produced by staurolite decomposition in quartz-free rocks and is related to the low-temperature part of the muscovite–sillimanite zone. The presence of andalusite together with sillimanite and spinel in reaction textures developing after staurolite (with sillimanite replacing andalusite) suggests that the *P–T* metamorphic trajectory passed close to the *And* ⟶ *Sil* transition line near the staurolite decomposition isograde.

The *P–T* metamorphic conditions of the metapelites of the sillimanite–muscovite zone can be estimated by the mineralogical garnet–cordierite, orthopyroxene–garnet, and garnet–biotite thermometry with the use of Samples 5257/23.2 and 5257/22, which contain garnet, biotite, cordierite, and orthopyroxene. The garnet–biotite thermometer yielded temperatures of 541–623°C, the garnet–orthopyroxene estimates are 552–560°C, and the garnet–cordierite temperatures are 642–683°C (Tables 11, 13), The pressures were estimated by the *Grt–Opx* barometer (Aranovich and Kosyakova, 1987; Harley, 1984) at 4.5–5.1 kbar (Table 12). The higher values of the garnet–cordierite temperatures seem to be caused by the not fully equilibrated character of garnet and cordierite in the metapelites and, hence, cannot be considered fully precise. The *P–T* metamorphic conditions of the K_2O-poor metapelites with the assemblage *Ol + Opx + Ged + Grt + Mag* (Sample 5267/290) were refined by the *Grt-Opx* thermometer, which yielded an interval of 544–639°C at a pressure of 4 kbar (Table 13). This rules out the possibility of the origin of this unusual mineral assemblage by a local heating, for example, near the contact with an intrusion.

Hence, the temperatures of the metamorphic zones were defined as follows: 530–554°C for the staurolite–sillimanite zone and 554–630°C for the muscovite–sillimanite zone at pressures of 4–5 kbar. It is hypothesized that the pressure decreased by 1–1.5 kbar at temperatures of 550–570°C, perhaps, because of the brief extension of the Prioskol'skaya structure during regional metamorphism.

CONCLUSION

The succession of mineral assemblages of K_2O-poor high-Al metapelites was described by several researchers (Korikovsky, 1979; Robinson *et al.*, 1982; Harley, 1985; and others). The medium-temperature region is dominated by assemblage with quartz, anthophyllite, gedrite, aluminum silicates, staurolite, and cordierite. A temperature increase results in the disappearance of staurolite from the assemblages according to the reaction *St + Qtz* ⟶ *Grt + Ged* + Al_2SiO_5. Under the *P–T* conditions of the muscovite–sillimanite facies, the *Ath + Ged + Crd* (often with garnet and/or sillimanite) assemblage becomes widespread. A further temperature increase up to the boundaries of the amphibolite and granulite facies is associated with the appearance of orthopyroxene in the mineral assemblages. Accord-

ing to Korikovsky (1979), orthopyroxene first appears in association with gedrite and then with sillimanite and cordierite. The decomposition of gedrite and origin of the orthopyroxene and cordierite assemblage by the reaction *Ged* ⟶ *Opx* + *Crd* + *Qtz* + H_2O roughly corresponds to the low-temperature boundary of the granulite facies (Korikovsky, 1979; Schreuers and Westra, 1985). In quartz-free rocks, gedrite can occur in association with sapphirine (Seifert, 1974; Lal *et al.*, 1978; and others).

Olivine appears in association with aluminous phases, such as cordierite (Herzberg, 1983; Anan'ev *et al.*, 1997; and others) and sapphirine (Grew *et al.*, 1994), owing to the reaction between enstatite and spinel. However, compared to the *En* + *Spl* assemblage, the assemblages *Ol* + *Crd* and *Ol* + *Sap* have narrower stability fields (Frost, 1975; Grew *et al.*, 1994).

Mineralogically, the sample bearing the *Ol* + *Ged* + *Grt* + *Opx* + *Mag* assemblage closely resembles aluminous low-Ca metaperidotites, whose phase equilibria are fairly well known and were reviewed by Tracy and Frost (1991). Metamorphism of these rocks results in the assemblage of olivine, orthopyroxene, spinel, and, sometimes, anthophyllite and hornblende, with the first mineral to crystallize being olivine (due to the decomposition of serpentine at temperatures as low as roughly 480°C, i.e., already within the staurolite zone).

Hence, in spite of their similar mineralogy, the quartz-free magnesian metapelites and metamorphosed ultramafics differ by both their mineral assemblages and the crystallization succession of minerals. This was likely caused by a combination of several factors: the bulk composition of the rocks (poor in K_2O, with moderate Al_2O_3 concentrations, and fairly magnesian quartz-free metapelite), metamorphic conditions (approximately 630°C and 5 kbar), and redox conditions (oxygen fugacity above the quartz–fayalite–magnetite buffer).

ACKNOWLEDGMENTS

We thank S.P. Korikovsky, Corresponding Member of the Russian Academy of Sciences, for valuable comments and constructive criticism expressed during the manuscript preparation. This study was financially supported by the Federal Program "Integration" (project no. S0007), Program "Russian Universities" (project no. 990087), a grant from the President of the Russian Federation (project no. 00-15-99397), and the Russian Foundation for Basic Research (project nos. 00-05-64522 and 01-05-06204).

REFERENCES

Abraham, K. and Shreyer, W., Petrology of a Ferruginous Hornfels from Rieckensgluk, Harz Mountains, Germany, *Contrib. Mineral. Petrol.*, 1973, vol. 40, pp. 275–292.

Anan'ev, V.A. and Reverdatto, V.V., The Fe-Apatite–Fe-Cordierite–Fayalite Unique Mineral Association in Ayu-Dag as a Result of Contact Metamorphism, *Dokl. Ross. Akad. Nauk*, 1997, vol. 353, no. 3, pp. 362–364.

Anan'ev, V.A., Sheplev, V.S., and Reverdatto, V.V., Thermodynamic Calculations of Mineral Equilibria and the Boundary of Contact Metamorphism for Fe-Rich Silica-Poor Metapelites, *Dokl. Ross. Akad. Nauk*, 1997, vol. 357, no. 5, pp. 665–666.

Arai, S., Contact Metamorphosed Dunite–Harzburgite Complex in the Chugoku District, Western Japan, *Contrib. Mineral. Petrol.*, 1975, vol. 52, pp. 1–16.

Aranovich, L.Ya. and Kosyakova, N.A., The Garnet–Orthopyroxene Geothermobarometer, Its Thermodynamics, and Application, *Geokhimiya*, 1987, no. 10, pp. 1363–1367.

Aranovich, L.Ya. and Podlesskii, K.K., Geothermobarometry of High-Grade Metapelites: Simultaneously Operating Reactions, in *Evolution of Metamorphic Belts*, Daly, J.S., Cliff, R.A., and Yardley, B.W.D., Eds., *Geol. Soc. Spec. Publ. London*, 1989, no. 43, pp. 45–61.

Aranovich, L.Ya. and Podlesskii, K.K., The Garnet–Plagioclase Geobarometer, *Dokl. Akad. Nauk SSSR*, 1980, vol. 251, no. 5, pp. 1216–1219.

Arnold, J. and Sandiford, M., Petrogenesis of Cordierite–Orthoamphibole Assemblages from the Springton Region, South Australia, *Contrib. Mineral. Petrol.*, 1990, vol. 106, pp. 100–109.

Bhattacharya, A., Krishnakumar, K.R., Raith, M., and Sen, S.K., An Improved Set of *a–X* Parameters for Fe–Mg–Ca Garnets and Refinements of the Orthopyroxene–Garnet Thermometer and the Orthopyroxene–Garnet–Plagioclase–Quartz Barometer, *J. Petrol.*, 1991, vol. 32, no. 3, pp. 629–656.

Chernyshov, N.M., Nenakhov, V.M., Lebedev, I.P., *et al.*, A Model for the Geodynamic Evolution of the Voronezh Massif in the Early Precambrian, *Geotektonika*, 1997, no. 3, pp. 21–30.

Chinner, G.A. and Fox, J.S., The Origin of Cordierite–Anthophyllite Rocks in the Land's End Aureole, *Geol. Magazine*, 1974, vol. 111, pp. 397–408.

Dobretsov, N.L., Reverdatto, V.V., Sobolev, V.S., *et al.*, *Fatsii metamorfizma* (Facies of Metamorphism), Moscow: Nedra, 1970.

Eskola, P., On the Petrology of the Orijärvi Region in Southwestern Finland, *Bulletin de la Comission Geologique de Finlande*, 1914, p. 40.

Ewans, B.W.D., Phase Relations of Epidote–Blueschists, *Lithos*, 1990, vol. 25, pp. 3–23.

Fischer, H., Schreyer, W., and Maresch, W.V., Synthetic Gedrite: A Stable Phase in the System $MgO–Al_2O_3–SiO_2–H_2O$ (MASH) at 800°C and 10 kbar Water Pressure, and the Influence of Fe, Na, Ca Impurities, *Contrib. Mineral. Petrol.*, 1999, vol. 136, pp. 184–191.

Fonarev, V.I., Graphchikov, A.A., and Konilov, A.N., A Consistent System of Geothermometers for Metamorphic Complexes, *Int. Geol. Rev.*, 1991, vol. 33, no. 8, pp. 743–783.

Frost, B.R., Contact Metamorphism of Serpentinite, Chloritic Blackwall, and Rodingite at Paddy-Go-Easy Pass, Central Cascades, Washington, *J. Petrol.*, 1975, vol. 16, pp. 272–313.

Gable, D.J. and Sims, P.K., Geology and Regional Metamorphism of Some High-Grade Cordierite Gneisses, Front Range, Colorado, *Spec. Paper Geol. Soc. Am.*, 1969, vol. 128.

Glagolev, A.A. and Boronikhin, V.A., Mineral Associations of High-Alumina Crystalline Schists from the Voron'i Tun-

dras, Kola Peninsula, *Izv. Akad. Nauk SSSR, Ser. Geol.*, 1977, no. 10, pp. 57–76.

Grant, J.A., Partial Melting of Common Rocks as a Possible Source of Cordierite–Anthophyllite-Bearing Assemblages, *Am. J. Sci.*, 1968, vol. 266, pp. 908–931.

Grew, E.S., Pertsev, N.N., Yates, M.G., *et al.*, Sapphirine–Forsterite and Sapphirine + Humite-Group Minerals in Ultra-Magnesian Lens from Kuhi-Lal, SW Pamirs, Tajikistan: Are These Assemblages Forbidden?, *J. Petrol.*, 1994, vol. 35, part 5, pp. 1275–1293.

Harley, S.L., Paragenetic and Mineral–Chemical Relationships in Orthoamphibole-Bearing Gneisses from Enderby Land, East Antarctica: A Record of Proterozoic Uplift, *J. Metamorph. Geol.*, 1985, vol. 3, pp. 179–200.

Harley, S.L., The Solubility of Alumina in Orthopyroxene Coexisting with Garnet in FeO–MgO–Al_2O_3–SiO_2 and CaO–FeO–MgO–Al_2O_3–SiO_2, *J. Petrol.*, 1984, vol. 25, no. 3, pp. 665–694.

Herzberg, C.T., The Reaction Forsterite + Cordierite = Aluminous Orthopyroxene + Spinel in the System MgO–Al_2O_3–SiO_2, *Contrib. Mineral. Petrol.*, 1983, vol. 84, pp. 84–90.

Hoffer, E. and Grant, J.A., Experimental Investigations of the Formation of Cordierite–Orthopyroxene Parageneses in Pelitic Rocks, *Contrib. Mineral. Petrol.*, 1980, vol. 73, pp. 15–22.

Holdaway, M.J. and Lee, S.M., Fe–Mg Cordierite Stability in High-Grade Pelitic Rocks Based on Experimental, Theoretical, and Natural Observations, *Contrib. Mineral. Petrol.*, 1977, vol. 63, no. 2, pp. 175–198.

Kamineni, D.S., Metasedimentary Cordierite–Gedrite Rocks of Archean Age near Yellowknife, Canada, *Precambrian Res.*, 1979, vol. 9, pp. 298–301.

Korikovsky, S.P., *Fatsii metamorfizma metapelitov* (Metamorphic Facies of Metapelites), Moscow: Nauka, 1979.

Lal, R.K., Ackermand, D., Seifert, F., and Haldar, S.K., Chemographic Relationships in Sapphirine-Bearing Rocks from Sonapahar, Assam, India, *Contrib. Mineral. Petrol.*, 1978, vol. 67, pp. 169–187.

Lavrent'eva, I.V. and Perchuk, L.L., Phase Equilibria in the Biotite–Garnet System: Experimental Data, *Dokl. Akad. Nauk SSSR*, 1981, vol. 260, no. 3, pp. 731–734.

Leake, B.E., Schumacher, J.C., Smith, D.C., *et al.*, Nomenclature of Amphiboles, *Mineral. Mag.*, 1997, vol. 42, pp. 625–640.

Lee, H.I. and Ganguly, J., Equilibrium Compositions of Coexisting Garnet and Orthopyroxene: Experimental Determinations in the System FeO–MgO–Al_2O_3–SiO_2, and Applications, *J. Petrol.*, 1988, vol. 29, no. 1, pp. 93–113.

Otten, M.T., Na–Al-Rich Gedrite Coexisting with Hornblende in a Corona between Plagioclase and Olivine, *Am. Mineral.*, 1984, vol. 69, pp. 458–464.

Perchuk, L.L., Consistency of Some Fe–Mg Geothermometers on the Basis of the Nernst Law: A Revision, *Geokhimiya*, 1989, no. 5, pp. 611–622.

Perchuk, L.L., Lavrent'eva, I.V., Kotelnikov, A.R., and Petrik, I., Comparative Characteristics of the Metamorphism Thermodynamic Regimes for Rocks of the Major Caucasian Range and Western Carpathian, *Geol. Zborn.—Geol. Carpatika*, 1984, vol. 35, no. 1, pp. 105–155.

Powell, R. and Holland, T., Calculated Mineral Equilibria in the Pelite System KFMASH (K_2O–FeO–MgO–Al_2O_3–SiO_2–H_2O), *Am. Mineral.*, 1990, vol. 75, pp. 367–380.

Reinhardt, J., Cordierite–Anthophyllite Rocks from Northwest Queensland, Australia: Metamorphosed Magnesian Pelites, *J. Metamorph. Geol.*, 1987, vol. 5, pp. 451–472.

Robinson, P. and Jaffe, H., The Composition Field of Anthophyllite and Fe-Anthophyllite Miscibility Gap, *Am. Mineral.*, 1970, vol. 55, pp. 307–3079.

Robinson, P., Klein, C., and Ross, M., Equilibrium Coexistence of Three Amphiboles, *Contrib. Mineral. Petrol.*, 1969, vol. 22, pp. 248–258.

Robinson, P., Ross, M., and Jaffe, H.W., Composition of the Anthophyllite–Gedrite Series, Comparisons of Gedrite and Hornblende, and the Anthophyllite–Gedrite Solvus, *Am. Mineral.*, 1971, vol. 56, pp. 1005–1041.

Robinson, P., Spear, F.S., Schumacher, J.S., *et al.*, Phase Relations of Metamorphic Amphiboles: Natural Occurrences and Theory, *Reviews in Mineralogy*, Mineral. Soc. Amer., 1982, vol. 9, pp. 1–227.

Sawaki, T., Cordierite–Olivine Symplectites in Fe–Al-Rich Hornfels from the Nogo–Hakusan Area, Gifu Prefecture, Central Japan, *J. Mineral. Petr., Econ. Geol.*, 1990, vol. 85, no. 6, pp. 270–281.

Schreuer, W. and Abraham, K., Three Stage Metamorphic History of a Whiteschist from Sar-e-Sang, Afghanistan, as a Part of a Former Evaporite Deposit, *Contrib. Mineral. Petrol.*, 1976, vol. 59, pp. 111–130.

Schreuers, J. and Westra, L., Cordierite–Orthopyroxene Rocks: The Granulite Facies Equivalents of the Orijarvi Cordierite–Orthoamphibole Rocks in West Uusimaa, Southwest Finland, *Lithos*, 1985, vol. 18, pp. 215–228.

Schumacher, J.C. and Robinson, P., Mineral Chemistry and Metasomatic Growth of Aluminous Enclaves in Gedrite–Cordierite Gneiss from Southwestern New Hampshire, USA, *J. Petrol.*, 1987, vol. 28, pp. 1033–1073.

Seifert, F., Stability of Sapphirine: A Study of the Aluminous Part of the System MgO–Al_2O_3–SiO_2–H_2O, *J. Geol.*, 1974, vol. 82, pp. 173–204.

Shchegolev, I.N., Il'yash, V.V., Lebedev, I.P., *et al.*, *Geologiya Prioskol'skogo mestorozhdeniya KMA*, (The Geology of Prioskol'skoe Deposit, Kursk Magnetic Anomaly), Available from VINITI, 1988, Moscow, no. 822-1388.

Smith, M.S., Symek, R.F., and Schneiderman, J.S., Implication of Trace Element Geochemistry for the Origin of Cordierite–Orthoamphibole Rocks from Orijarvi, SW Finland, *J. Geol.*, 1992, vol. 100, pp. 545–559.

Spear, F.S. and Cheney, J.T., A Petrogenetic Grid for Pelitic Schists in the System SiO_2–Al_2O_3–FeO–MgO–K_2O–H_2O, *Contrib. Mineral. Petrol.*, 1989, vol. 101, no. 29, pp. 149–164.

Spear, F.S., The Gedrite–Anthophyllite Solvus and the Composition Limits of Orthoamphibole from the Post Pond Volcanics, Vermont, *Am. Mineral.*, 1980, vol. 65, pp. 1103–1118.

Stoddard, E.F. and Miller, C., Chemistry and Phase Petrology of Amphiboles and Orthoamphibole–Cordierite Rocks, Old Woman Mountains, SE California, USA, *Mineral. Mag.*, 1990, vol. 54, pp. 394–406.

Thompson, A.B., Mineral Reactions in Pelitic Rocks: 1. Prediction of *P–T–X* (Fe–Mg) Relations, *Am. J. Sci.*, 1976, vol. 276, no. 4, pp. 401–424.

Tilley, C.E. and Fleet, J.S., Hornfelses from Kenidjak, *Geol. Surv. of Great Britain, Summary of Progress Report II*, 1929, pp. 24–41.

Tracy, R.J. and Frost, B.R., Phase Equilibria and Thermobarometry of Calcareous, Ultramafic and Mafic Rocks, and Iron Formations, *Rev. Mineral., Contact Metamorphism*, 1991, vol. 26, pp. 207–289.

Will, T., Okrusch, M., Schmadicke, E., *et al.*, Phase Relations in the Greenschist–Blueschist–Amphibolite–Eclogite Facies in the System Na_2O–CaO–FeO–MgO–Al_2O_3–SiO_2–H_2O (NCFMAS) with Application to Metamorphic Rocks from Samos, Greece, *Contrib. Mineral. Petrol.*, 1998, vol. 132, no. 1, pp. 85–102.

Will, T.M., Powell, R., and Holland, T., A Calculated Petrogenetic Grid for Ultramafic Rocks in the System CaO–FeO–MgO–Al_2O_3–SiO_2–CO_2–H_2O at Low Pressure, *Contrib. Mineral. Petrol.*, 1990, vol. 105, pp. 347–358.

Xu, G., Will, T.M., and Powell, R., A Calculated Petrogenetic Grid for the System K_2O–FeO–MgO–Al_2O_3–SiO_2–H_2O with Particular Reference to Contact-Metamorphosed Pelites, *J. Metamorph. Geol.*, 1994, no. 12, pp. 99–119.